

THESIS

A COMPARITIVE STUDY BETWEEN VECTOR CONTROL AND DIRECT TORQUE
CONTROL OF INDUCTION MOTOR USING MATLAB SIMULINK

Submitted by

Fathalla Eldali

Department of Electrical and Computer Engineering

In partial fulfillment of the requirements

For the Degree of Master of Science

Colorado State University

Fort Collins, Colorado

Fall 2012

Master's Committee:

Advisor: George J. Collins

Siddharth Suryanarayanan
Hiroshi Sakurai

Copyright by Fathalla Eldali 2012

All Rights Reserved

ABSTRACT

A COMPARITIVE STUDY BETWEEN VECTOR CONTROL AND DIRECT TORQUE CONTROL OF INDUCTION MOTOR USING MATLAB SIMULINK

This thesis project studies and compares two of the most commonly used electric driving methods of induction motors (IM). These methods, which have been used for three decades are Field Orientation Control (FOC) and Direct Torque Control (DTC). Theoretical background for both methods is explained. Due to its simplicity of use, MATLAB/ SIMULINK is used to simulate the dynamic model of (IM) and applying both techniques on it. The comparative study of speed, torque, and flux is performed under two cases which are the normal operation and in the presence of voltage-sag and short interruption.

ACKNOWLEDGEMENTS

I would like to thank and appreciate the effort which was done by my advisor Dr. George Collins and the ECE Department at Colorado State University for allowing me the privilege and opportunity of doing a thesis at Colorado State University. Dr. Collins' expertise, understanding, and patience have strongly contributed to my thesis.

I would also like to thank my loving family for their support, motivation and help. Without the support and encouragement of my family, and friends I would never have finished my degree.

Last, I would like to thank my committee members to help by their suggestions and notes and special thanks to Dr. Siddharth Suryanarayanan who taught me power quality class and that gave me the opportunity to add a very interesting part to my thesis project.

DEDICATION

To my father, Abdullateef, to the soul of my mother, my brothers and sisters. Without your help, support, and patience, I could not have done this effort

TABLE OF CONTENTS

ABSTRACT.....	ii
ACKNOWLEDGEMENTS.....	iii
DEDICATION.....	iv
LIST OF TABLES.....	vii
LIST OF FIGURES.....	viii
CHAPTER 1	
INTRODUCTION.....	1
1.1 Introduction of Project.....	1
1.2 Literature Review.....	2
1.3 Thesis chapters overview and thumbnail sketches of contents.....	5
CHAPTER 2	
DYNAMIC MODELING OF THREE PHASE INDUCTION MOTOR.....	7
2.1 Introduction.....	7
2.2 Induction motor construction, principles and operation.....	8
2.3 Induction Motor Drive.....	9
2.4 Mathematical Representation of Three Phase Induction Motor.....	11
2.4.1 Three Phase Induction Machines.....	11
2.4.2 Machine Model in Arbitrary Reference Frames.....	14
CHAPTER 3	
EXPLANATION OF TWO INDUCTION MOTOR DRIVES VECTOR CONTROL VS. DIRECT TORQUE CONTROL.....	18
3.1 Introduction.....	18
3.2 Vector Control of Induction Motor.....	19
3.2.1 Torque in separately excited dc motor.....	19
3.2.2 Principles of vector control of Induction motor.....	21
3.2.3 Torque equations for Vector Control.....	22
3.2.4 Methods of Vector Control.....	24
3.3 Direct Torque Control.....	27
3.3.1 The Basic Principles of Direct Torque Control of Induction Motor.....	28
3.3.2 Space Vector Modulation of Three Phase Voltage Source Inverter with DTC.....	29
3.3.3 Basic principles of Switching Table.....	30
3.4 Theoretical Comparison Vector Control and Direct Torque Control.....	34
CHAPTER 4	
SIMULATION, RESULTS AND DISCUSSION.....	36
4.1 Introduction.....	36
4.2 Mathematical model simulation using MATLAB/ SIMULINK.....	36
4.2.1 Three phase to d-q stationary reference frame.....	37

4.2.2 d-q stationary frame to d-q synchronous frame	37
4.2.3 Electromagnetic Torque Equation modeling	38
4.3 Field Orientation Control (FOC) using MATLAB/ SIMULINK	42
4.4 Direct Torque Control (DTC) using MATLAB/ SIMULINK	43
4.5 Simulation Results	45
4.5.1 Simulation Results in the normal operation case	46
4.5.2 Simulation Results in the presence of Voltage-Sag and Short Interruption	55
CHAPTER 5	
CONCLUSION AND FUTUER WORK	62
5.1 Conclusion	62
5.2 RECOMMENDED FUTURE WORK	64
REFERENCES	65
Appendix A	
Induction Motor parameters.....	68
Appendix B	
The SIMULINK model of the Field Orientation Control (FOC) of Induction Motor.....	69
Appendix C	
Switching Table Code.....	70
Appendix D	
The SIMULINK model of Direct Torque Control (DTC) of Induction Motor.	72
Appendix E	
The Variation of DC link voltage, speed and motor current due to the Voltage Sag (Type A) and short interruption at different durations in both techniques.....	73

LIST OF TABLES

Table3.1 The effect of the voltage vector on the stator flux vector in Sector I	32
Table 3.2 Switching table of inverter vector voltages	33

LIST OF FIGURES

Figure 2.1 Induction motor rotor types.....	9
Figure 2.2 Idealized circuit model of three phase induction machine.....	13
Figure 2.3 Relationship between ABC and qdo arbitrary coordinate reference frames.....	15
Figure 3.1 Simple representation of separately excited DC motor.....	20
Figure 3.2 Principles of vector control	21
Figure 3.3 The Block diagram of direct vector control of Induction motor.....	26
Figure 3.4 Block diagram of indirect vector control of Induction motor.....	27
Figure 3.5 Circuit Diagram of Three phase Voltage Source Inverter.....	29
Figure 3.6 Three phase square-wave forms which is produced by the inverter.....	30
Figure 3.7 Illustrative Phase Voltages in Space Vector.....	30
Figure 3.8 Hysteresis bands for the stator flux and the electromagnetic torque.....	31
Figure 3.9 The hysteresis band controls the stator flux voltage and Torque.....	32
Figure 3.10 Block diagram of the Direct Torque Control of Induction motor.....	34
Figure 4.1 Three phase to d-q stationary frame transformation.....	37
Figure 4.2 Transformation from d-q stationary frame to d-q synchronous frame.....	38
Figure 4.3 Electromagnetic Torque.....	39
Figure 4.4 The mechanical output of the induction motor Model.....	39
Figure 4.5 Complete SIMULINK model of three phase Induction Motor.....	41
Figure 4.6 obtaining the reference $i_{d_s}^{e*}$ and $i_{q_s}^{e*}$ through the rotor flux and the speed error.....	42
Figure 4.7 transforming the two components of stator current from synchronous reference frame to stationary reference frame.....	43
Figure 4.8 d-q stationary reference frame to the reference three phase currents.....	43

Figure 4.9 The function of the Hysteresis controllers using Relays.....	44
Figure 4.10 Interpreted MATLAB Fcn is representing the switch table logic.....	45
Figure 4.11 Reference motor Speed (rpm) Vs. Time (sec).....	46
Figure 4.12 Motor speed response.....	48
Figure 4.13 Electromagnetic Torque.....	49
Figure 4.14 Stator Flux Response.....	50
Figure 4.15 Three phase motor current.....	52
Figure 4.16 Torque response.....	54
Figure 4.17 The distortion of Three phase current.....	54
Figure 4.18 Single Phase under Voltage Sag Conditions.....	57
Figure 4.19 Voltage Sag Phasor Diagrams.....	58
Figure 4.20 The effect of the duration of the three phase short interruption on DC Voltage.....	59
Figure 4.21 One phase short interruption's effect on DC link voltage.....	60
Figure 4.22 DC voltage wave shape under the effect of two types of voltage sag condition.....	60

CHAPTER 1

INTRODUCTION

1.1 Introduction of Project

Mechanical energy is needed in the daily life use as well as in the industry. Induction motors play a very important role in both worlds, because of low cost, reliable operation, robust operation and low maintenance. There are two main types of induction motors which are the wounded rotor and squirrel-cage design and both of them are in widespread use. Squirrel-cage rotor winding design is considered of the two more reliable and cheaper to make.

When induction motors are operated without a proper control (drive), the motors are consuming large energies and the operating costs are high. In last few decades, power electronics has emerged, Digital signal Processing (DSP) and microcontrollers are now well established, motion and I-V sensors are ubiquitous allowing improved the performance. The contribution of power electronics in driving the AC motors which is so called “adjustable speed drives”, is characterized by the three phase mains voltages being converted to DC through conventional rectifier circuits to a DC rail.

Next to the DC rail is inverted to AC but with both a different voltage and different frequency, V_{OUT} (f_{OUT}). Because the motor speed depends on the applied frequency, speed control is facilitated. The DC to AC inverter is usually built using Pulse Width Modulation (PWM) methodology to piecewise simulate the desired $V(f)$. DSP is considered a very important component in recording and analyzing the PWM I-V data from motion and I-V sensors and to compare it with the desired conditions in the motor controller. Dynamic models (mathematical models) are employed in to better understand the behavior of induction motor in both transient and steady state. The dynamic modeling sets all the mechanical equations for the inertia, torque and speed versus time. It also models all the differential voltage, currents and flux linkages

between the stationary stator as well as the moving rotor. My mathematical model will be done using MATLAB/Simulink which will represent the three phase induction motor including a three phase to d-q axis transformations. The main benefit with MATLAB Simulink is that in the electromechanical dynamic model can be accomplished in a simple way and it can be simulated faster using function blocks.

Hasse in 1969 and *Blaschke* in 1972 proposed the concept of the vector control method or so called Field Orientation method of AC motors, based on making the well-established separately excited dc machine. Here the torque is defined as the cross vector product of the magnetic field from the stator poles and the armature current. To a good approximation the two are perpendicular, thus the maximum torque can be achieved and independent control of the motor facilitated. This is why vector control is often called “decoupling control”.

Direct Torque Control concepts were proposed by Takashi and Noguchi in 1986. The idea of this method is based on comparing the measured stator flux and torque with the theoretically desired bands. The vector differences will control the subsequent switching sequence of the SVPWM inverter voltage based on the switching logic table. That however restricts the means the stator flux and torque to fall in the pre-established bands.

1.2 Literature Review

To ground this thesis, many prior art research papers have been read to distilled into three main topic points. First, understanding and modeling the performance of the uncontrolled induction motor, and especially the dynamic (mathematical) representation via MATLAB/SIMULINK for the dynamic electromechanical coupled equations and studying the assumptions in the modeling procedure of Field Orientation Control (FOC). Finally, Direct Torque Control methodologies were studied using different analytic techniques.

The importance of the equivalent electrical circuit of three phase induction machine in dynamic modeling has been explained in [13] as well as the utility of the d-q transformations. Those transformations can be done in three main reference frames which are stationary at (start-up), synchronous (at steady state) and rotor reference frame (during speed changes) as shown in [10]. Stationary and synchronous reference frames are the most common used. The representation of the mathematical model in different reference frames are explained as well as the step by step procedure of established MATLAB/SIMULINK rotational dynamic models illustrating the simplicity of using SIMULINK[12], [7].

The basic idea of Vector control for induction motor control is explained in both reference frames in [8] and [11]. The latter paper explains vector control concepts allowing the induction motor, to behave as a simple separately excited DC motor. It also details the established motor control method, the “scalar control method”, which controls only the magnitude of the voltage with a fixed frequency. This paper also derives the torque equations and then explains the two different ways of applying this control method in many different motor classifications. Finally, it compares actual and simulation results. A different approach, a fuzzy controller, was introduced in [11], where the of Vector Control method provided in differences between measured and simulated data for input to the PI controller in torque control loop. The disadvantage of the Field Orientation Control is that this method is sensitive to the changing dynamic parameters, being dependant on the rotor time constant [8]. FOC or, decoupling control, employs a clever mathematical coordinate transformation, to convert the three phase ac to two orthogonal dc components. The abc to d-q transformation, which is called Clarke Transformation, and vice versa, which is called inverse Clarke Transformation, are explained

and modeled using SIMULINK [9]. In this way one can decouple the stator flux and the torque so they can be separately controlled.

Induction motor drives may be classified into two main control strategies. Scalar control, of the voltage magnitude and frequency is one. A second is controlling both the voltage vector and the frequency, which can be FOC or Direct Torque Control (DTC). In the research papers [16],[17] DTC principles are introduced, which allow keeping the flux and the torque falling in pre-established bands and using the hysteresis control via a switching table. The idea of Space Vector pulse Width Modulation (SV-PWM) which is used to defined the state of the inverter switching and the voltage vector. SVM is explained in detail in [14] and modeled using MATLAB. Another comparative study was conducted [15] to explore the difference between the conventional DTC and the DTC adding a PI controller, which is used in this thesis to get better reduction the ripple in the resultant flux and torque.

One motivation for doing this thesis as a comparative study between FOC and DTC, is that few research papers were published on this topic as a comparative study and I judged it was ripe for a detailed study to explore future control approaches. As Many papers, on the other hand, were written about DTC and FOC individually and using many types of controllers trying to improve the performance of those methods of motor control. The other motivation is that all those papers and studies were done based on the performance comparison only assuming that everything is in normal operation which is not always the case. Therefore, two power quality issues are included in these comparison studies which are the voltage sag and short interruption.

A theoretical comparative study between the DTC on one hand and other methods of motor drive has been done [18], explaining the basic principles of DC drive, scalar control, flux vector control, as well as direct torque control. Another comparative study between FOC and

DTC outlined the characteristics of the control algorithms, dynamic electromechanical response, and the sensitivity analysis of changing parameters in the implementation [19]. The latter paper uses Simulink in the comparison as was the inspiration for this thesis except this paper used the built in induction motor block which is different than what I used as a mathematical model to get more precise results in the case of unbalanced voltage and parameters changing. Finally the last prior work, [20], focuses on the similarities between FOC and DTC by reexamining the basic principles between both and studying how combine the two to make a both more accurate and faster control algorithm. Based on that, this study has been compared with the other studies and the comparison has added more comparison aspects.

1.3 Thesis chapters overview and thumbnail sketches of contents

In Chapter 2 the thesis gives a brief background about induction motor electrical and mechanical construction, a theoretical and mathematical description of induction motors that includes the differential equations in both reference frames(stationary and synchronous) and the mathematical required transformations between the two. This chapter explains also the practical needs of dynamically driving induction motors.

Chapter 3 introduces and explains the Vector Control method starting from the basic ideas, outlining the object of using this analysis and control technique to better control and drive induction motors. The advantages and disadvantages of using Vector control method are outlined.

The second established technique of induction motor control is also introduced in Chapter 3, which is the Direct Torque control method, and the details for the proper design and implementation. It also introduces how the model is constructed and operated including the logic switching table and sequence.

Chapter 4 presents my Simulink model for the induction motor first and then the models for both Vector Control and Direct Torque Control in details. It is employed for the simulation results and detailed comparison with each. The result of this comparison is presented.

In Chapter 5 gives the conclusion and some recommendations for future works employing Simulink and experimental study.

CHAPTER 2

DYNAMIC MODELING OF THREE PHASE INDUCTION MOTOR

2.1 Introduction

Nikola Tesla first developed the principles of multi-phase AC motors in 1888. Because an induction motor is less expensive to make, is electrically and mechanically robust, and it operates broad range of speed, torque and mechanical power, it is the most commonly used motor in industry. It is available from several watts single phase small motor designs, induction motors evolved to tens thousands of horse power (746 Watts/HP) driven by three phase mains voltages.

In general, induction motors consist of two main parts which are: the stator which carries the field winding, which is connected single or multi-phase voltage source, and which creates the rotating magnetic field between stator and rotor. The rotor winding is short circuited or connected to an external variable resistance for motor speed control purposes [3], especially during start-up where large torques are required. Unlike the DC separately excited and synchronous machines, induction motors are supplied through the rotating stator magnetic field, which makes the construction simple and reliable. There are two types of rotor windings, are wounded rotor and squirrel-cage rotor. The latter is less expensive and more robust. Everything in this thesis project is based solely on the squirrel-cage induction motor approach [1] [6].

In this chapter, induction motor electrical and mechanical construction is detailed. The rotating field concept is explained and then the induction motor circuit model is also explained. Using the circuit models and the mechanical equations of motion with motor moment of inertial mathematical (Dynamic) equations of motion from start-up, through steady state operation as well as changing speed conditions are derived and presented. All work employs

MATLAB/Simulink and introduces the reader to my methodology which is explained in details in chapter 4.

2.2 Induction motor construction, principles and operation

The induction machine can be operated as a motor or a generator. The selection of the motor mode requires understanding the various types of induction motor squirrel cage winding choices. Induction of voltages between the rotor and stator depends on mechanical design, primarily air gap geometries between the static stator and moving rotor. Rotor geometry and materials choice determine the rotor moment of inertia, for dynamical mechanical modeling.

In general, three phase AC machines have similar construction. The stator is usually made of laminated sheet steel (to reduce eddy current losses) which is attached to an iron frame. This stator consists of mechanical slots of high aspect ratio (height to width ratios) to bury the insulated copper conductors inside the stator structure, and then the stator conductors are connected in three phase delta or wye configurations.

The wire wound rotor contains three electrical phases just as the stator does and they (coils) are connected wye or delta. The electrical terminals are connected to the slip rings. Unlike the wire wound, the squirrel-cage's rotor contains bars of aluminum or copper imbedded in the rotor, which are short circuited at the end of each bar by an end disc thereby placing all rotor wires in parallel and placed equally spaced around the Rotor circumference. The wire wound rotor and squirrel-cage rotor are each shown in Fig. 2.1 for comparison.

Under normal operation, an induction motor runs at a speed which is lower than the synchronous speed, so that a time changing magnetic field is created to couple stator and rotor windings. At start up this time varying magnetic field is maximized geometrically, but at near synchronous speed the time derivative is reduced. Therefore operating the motor at a rotor speed

which is close to the synchronous speed of the stator magnetic field makes the motor self-limit according to the difference of the motor and load torques. The synchronous motor speed is directly proportional to the input AC line frequency driving the stator fields and inversely proportional with the number of magnetic poles, created in the stator by the choice of stator winding coil positions. Motor speed is given in equations 2.1 and 2.2

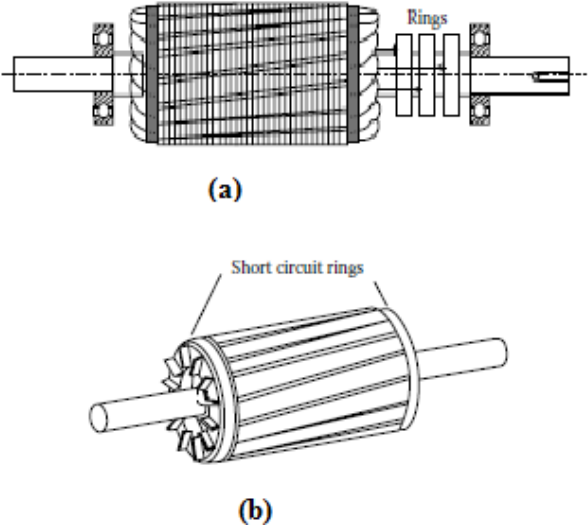


Figure 2.1 Induction motor rotor types (a) Wounded rotor (b) Squirrel-Cage rotor.

It was taken without permission from [22]

$$N_S = \frac{120 f}{P} \tag{2.1}$$

$$\omega_S = \frac{2\pi N_S}{60} = \frac{4\pi f}{P} \tag{2.2}$$

2.3 Induction Motor Drive

Squirrel-cage induction motors are the standard of industry. They are rated at a given operating speed and operating torque, setting the power level available at the load. Motor

efficiency then determines the required input AC power. When rotors are revolving at a speed close to the stator synchronous speed of the rotating magnetic field they are efficient in creating enough torque due to the low dB/dt seen by the rotor wires and hence the low induced rotor wire currents.

In many practical applications the induction motor doesn't work at its rated speed. For example, in air conditioning systems, where the fan is an induction motor, the fan works only till the temperature reaches the desired value. Switching the fan (motor) on and off is possible but mechanically stressful. So operating the induction motor by decreasing the rotation speed when it is not needed is a better way to save energy and reduce mechanical stress [21]. Motor speed control via variable frequency voltage drives, $V(f)$ is natural.

There are two main classifications of induction motor control drives depending on the type of motor application:

1. Adjustable-speed drives: these are used in applications which the control of the motor speed is of primary concern such as: fans, blower, grinders and so on.
2. Servo drives: these deal with advanced control, such as in robotics where simultaneous torque, speed, and position control are sought [5].

Both the frequency of the variable voltage drive and the voltage level can be varied using power electronic converters such as Adjustable Speed Drive (ASD) or Variable Frequency Speed Drive (VFD). A VFD is the focus of this thesis project.

An efficient creation of $V(f)$ from a DC rail via inverter methods leads to better energy conservation, as the torque of an induction motor varies as shown in Equation 2.3.

$$\text{Torque} \approx k_1(\text{speed})^2 \quad (2.3)$$

Applying the correct frequency controls the rotation speed and thereby the torque needed by the mechanical load. The mechanical load power equals the torque multiplied by the speed so the load power is as shown in equation 2.4

$$\text{Power} \simeq k_2(\text{speed})^3 \quad (2.4)$$

Where k_1 and k_2 are the constants of proportionality, are specified empirically, and depend on the wiring choices and wiring geometries employed in both the stator and rotor designs.

Speed control controls motor power consumption and can be optimized to improve the overall efficiency of motor-mechanical load systems as we show below in detailed mathematical modeling.

2.4 Mathematical Representation of Three Phase Induction Motor

The proper modeling each induction machine is a key to apply the most efficient drive methods to the stator windings. Mathematical modeling allows the engineer to better select the best suited mathematical coordinate system transformations. Those coordinate transformations are choices are outlined in this section as well.

2.4.1 Three Phase Induction Machines

The equivalent circuit model of three phase AC machines is shown in Fig. 2.2 where the three phases of the stator and the rotor are both modeled by inductive components and appropriate AC voltage sources. The stator three phase input voltages, from the artificial V (f) mains, are given in equations 2.5 as well as the induced rotor three phase voltages which are given in equations 2.6.

$$\begin{aligned}
v_{as} &= i_{as}r_s + \frac{d\lambda_{as}}{dt} V \\
v_{bs} &= i_{bs}r_s + \frac{d\lambda_{bs}}{dt} V \\
v_{cs} &= i_{cs}r_s + \frac{d\lambda_{cs}}{dt} V
\end{aligned} \tag{2.6}$$

The magnetically induced rotor three phase voltages in the rotor coils are:

$$\begin{aligned}
v_{ar} &= i_{ar}r_r + \frac{d\lambda_{ar}}{dt} V \\
v_{br} &= i_{br}r_r + \frac{d\lambda_{br}}{dt} V \\
v_{cr} &= i_{cr}r_r + \frac{d\lambda_{cr}}{dt} V
\end{aligned} \tag{2.7}$$

The flux linkage equations between the stator and rotor (via L_{ss}^{abc} and L_{rr}^{abc}) as well as leakage fluxes via the mutual inductances L_{sr}^{abc} and L_{rs}^{abc} are given in condensed matrix notation form in matrix equation 2.8

$$\begin{bmatrix} \lambda_s^{abc} \\ \lambda_r^{abc} \end{bmatrix} = \begin{bmatrix} L_{ss}^{abc} & L_{sr}^{abc} \\ L_{rs}^{abc} & L_{rr}^{abc} \end{bmatrix} \begin{bmatrix} i_s^{abc} \\ i_r^{abc} \end{bmatrix} \text{ Wb. turn} \tag{2.8}$$

The circuit model of the induction motor will have six independent inductances as outlined below. Three are for the stator and three are for the rotor. Where L_{ss} is a single equivalent stator wire coil inductance and a corresponding single equivalent rotor inductance L_{rr} . In addition the model has three additional components which are per phase leakage inductance L_{ls} and L_{rs} , self-inductance L_{ss} and L_{rr} as well as mutual inductance L_{sm} and L_{rm} respectively as given in equations 2.9 and 2.10.

$$L_{ss}^{abc} = \begin{bmatrix} L_{ls} + L_{ss} & L_{sm} & L_{sm} \\ L_{sm} & L_{ls} + L_{ss} & L_{sm} \\ L_{sm} & L_{sm} & L_{ls} + L_{ss} \end{bmatrix} H \tag{2.9}$$

$$L_{rr}^{abc} = \begin{bmatrix} L_{lr} + L_{rr} & L_{rm} & L_{rm} \\ L_{rm} & L_{lr} + L_{rr} & L_{rm} \\ L_{rm} & L_{rm} & L_{lr} + L_{rr} \end{bmatrix} H \tag{2.10}$$

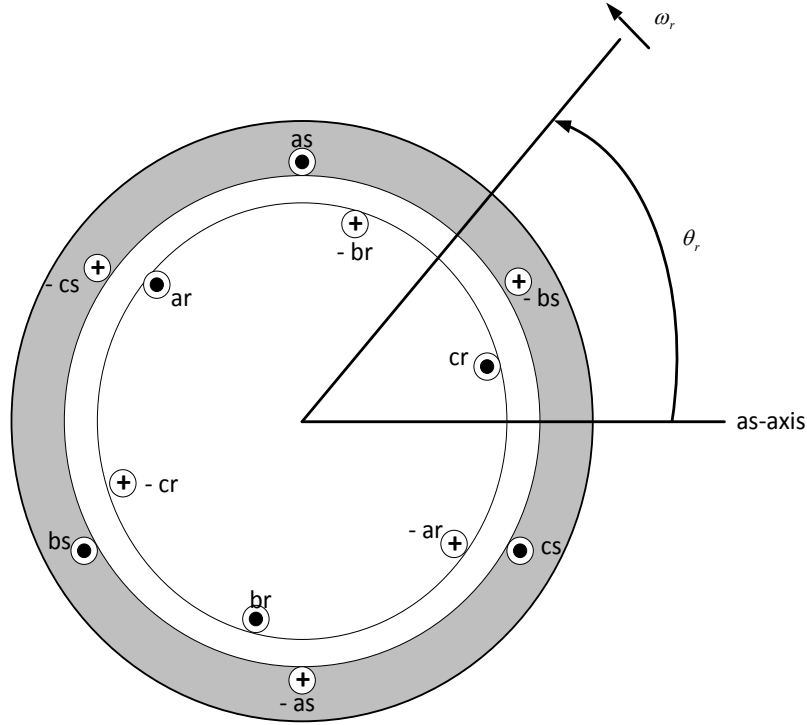


Figure 2.2 Idealized circuit model of three phase induction machine, showing the rotating stator magnetic field and the mechanically rotating rotor.

Reproduced without permission from [2]

The rotor to stator mutual inductance, L_{sr}^{abc} , depends on the rotor position (θ_r) with respect to the various stator coils and associates magnetic poles, as given in equation in matrix form 2.11

$$L_{sr}^{abc} = [L_{rs}^{abc}]^t = L_{sr} \begin{bmatrix} \cos \theta_r & \cos \left(\theta_r + \frac{2\pi}{3} \right) & \cos \left(\theta_r - \frac{2\pi}{3} \right) \\ \cos \left(\theta_r - \frac{2\pi}{3} \right) & \cos \theta_r & \cos \left(\theta_r + \frac{2\pi}{3} \right) \\ \cos \left(\theta_r + \frac{2\pi}{3} \right) & \cos \left(\theta_r - \frac{2\pi}{3} \right) & \cos \theta_r \end{bmatrix} H \quad (2.11)$$

The three phase induction machine is therefore represented in circuit form by employing the six independent and distinct stator and rotor equations in 2.6 and 2.7 respectively.

The flux linkage that enters into the air gap region, has two parts and the mutual inductance between the rotor and stator is depending on the rotor position, so it is depended on the rotor angle (θ_r).That means the rotor and stator equations are depending on each other

(mutual coupling). To make the dynamic induction motor model easier, clever mathematical transformations or mappings between coordinate systems are used, which is explained in the next section [2], [24].

2.4.2 Machine Model in Arbitrary Reference Frames

There are three main reference frames of motion, which could be used to model the three phase induction machine in its three main regions of operation. These are the stationary reference frame for startup, the synchronous reference frame for equilibrium motion, and the rotor reference frame for changing speeds by acceleration or deceleration. The two commonly employed coordinate transformations with induction machine are the stationary and the synchronous reference frame. These mathematical transformations, which are known as Park Transformation [10], can facilitate understanding of the variation of the mutual inductance between the stator and the rotor under differing rotation conditions. Referring to Fig. 2.3, and deriving the equations for three phase induction machine in arbitrary reference frame with the speed ω in the same direction of rotor rotation. This arbitrary frame can then be specified as stationary or synchronous. When $\omega = 0$, this means the reference frame does not move (stationary) and this transformation is commonly used in Adjustable Speed Drives. Similarly, when the reference frame is revolving in the synchronous speed, the reference frame can be represented in synchronous reference frame. This is a representation used to simulate power system components.

By applying rotating coordinate transformations to the stator and rotor voltages, current and flux linkage equations, which are represented in equations 2.6-2.11 respectively, those equations can be represented in simpler form by proper choice of reference frames.

$$\begin{bmatrix} f_q \\ f_d \\ f_0 \end{bmatrix} = [T_{qdo}(\theta)] \begin{bmatrix} f_a \\ f_b \\ f_c \end{bmatrix} \quad (2.12)$$

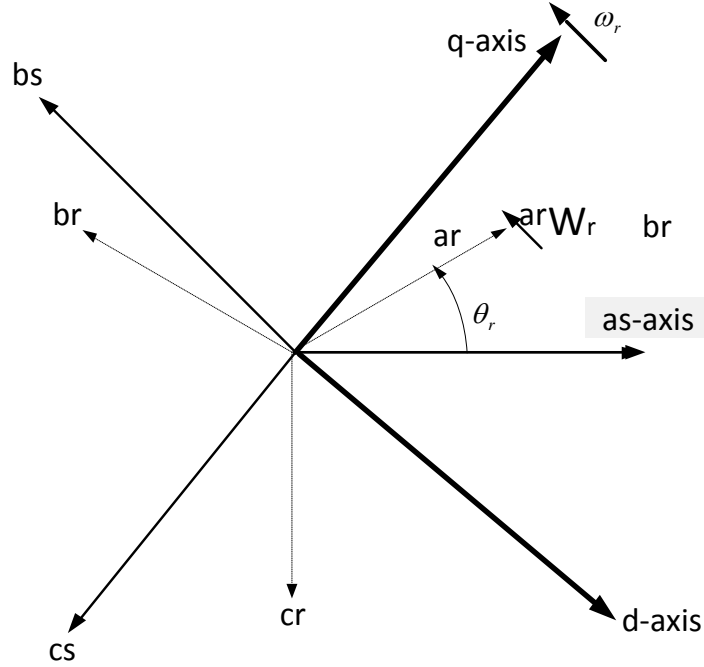


Figure 2.3 Relationship between ABC and qdo arbitrary coordinate reference frames.

Recreated directly without permission from [2]

Where f can be stator or rotor voltage, current as well as a flux linkage of the stator or rotor of the induction machine, located in the air gap region between stator and rotor. $T_{qdo}(\theta)$ is the associated torque transformation matrix.

$$T_{qdo}(\theta) = \frac{2}{3} \begin{bmatrix} \cos \theta & \cos \left(\theta - \frac{2\pi}{3} \right) & \cos \left(\theta + \frac{2\pi}{3} \right) \\ \sin \theta & \sin \left(\theta - \frac{2\pi}{3} \right) & \sin \left(\theta + \frac{2\pi}{3} \right) \\ \frac{1}{2} & \frac{1}{2} & \frac{1}{2} \end{bmatrix} \quad (2.13)$$

The inverse of the transformation matrix obtained by matrix methods and is:

$$[T_{qdo}(\theta)]^{-1} = \begin{bmatrix} \cos \theta & \sin \theta & 1 \\ \cos \left(\theta - \frac{2\pi}{3} \right) & \sin \left(\theta - \frac{2\pi}{3} \right) & 1 \\ \cos \left(\theta + \frac{2\pi}{3} \right) & \sin \left(\theta + \frac{2\pi}{3} \right) & 1 \end{bmatrix} \quad (2.14)$$

2.4.2.1 qdo Stationary Reference Frame Equations Applicable for Motor Start Up conditions

In summary we list below the various voltages in the stator and rotor as well as the flux linkages which determine the various shaft torques in the “stationary qdo reference frame”.

$$\begin{aligned}
 & \text{Stator and Rotor Voltages} \\
 & v_{qs}^s = \frac{p}{\omega_b} \psi_{qs}^s + r_s i_{qs}^s \\
 & v_{ds}^s = \frac{p}{\omega_b} \psi_{ds}^s + r_s i_{ds}^s \\
 & v_{0s} = \frac{p}{\omega_b} \psi_{0s} + r_s i_{0s} \\
 & v_{qr}^s = \frac{p}{\omega_b} \psi_{qr}^s - \frac{\omega_r}{\omega_b} \psi_{dr}^s + r_r' i_{qr}^s \\
 & v_{dr}^s = \frac{p}{\omega_b} \psi_{dr}^s - \frac{\omega_r}{\omega_b} \psi_{qr}^s + r_r' i_{dr}^s \\
 & v_{0r} = \frac{p}{\omega_b} \psi_{0r} + r_r' i_{0r}
 \end{aligned} \tag{2.15}$$

Flux Linkage Equations in Matrix Notification

$$\begin{bmatrix} \psi_{qs}^s \\ \psi_{ds}^s \\ \psi_{0s} \\ \psi_{qr}^s \\ \psi_{dr}^s \\ \psi_{0r} \end{bmatrix} = \begin{bmatrix} x_{ls} + x_m & 0 & 0 & x_m & 0 & 0 \\ 0 & x_{ls} + x_m & 0 & 0 & x_m & 0 \\ 0 & 0 & x_{ls} & 0 & 0 & 0 \\ x_m & 0 & 0 & x_{lr}' + x_m & 0 & 0 \\ 0 & x_m & 0 & 0 & x_{lr}' + x_m & 0 \\ 0 & 0 & 0 & 0 & 0 & x_{lr}' \end{bmatrix} \begin{bmatrix} i_{qs}^s \\ i_{ds}^s \\ i_{0s} \\ i_{qr}^s \\ i_{dr}^s \\ i_{0r} \end{bmatrix} \tag{2.16}$$

Torque Equations

$$\begin{aligned}
 T_{em} &= \frac{3}{2} \frac{P}{2\omega_b} (\psi_{qr}^s i_{dr}^s - \psi_{dr}^s i_{qr}^s) \text{ N.m} \\
 T_{em} &= \frac{3}{2} \frac{P}{2\omega_b} (\psi_{ds}^s i_{qs}^s - \psi_{qs}^s i_{ds}^s) \\
 T_{em} &= \frac{3}{2} \frac{P}{2\omega_b} x_m (i_{dr}^s i_{qs}^s - i_{qr}^s i_{ds}^s)
 \end{aligned} \tag{2.17}$$

2.4.2.2 qdo Synchronous Reference Frame Equations Applicable for Near Synchronous Equilibrium Motor Operation

For comparison we list below the various voltages in the stator and rotor as well as the flux linkages which determine the various shaft torques in the “synchronous rotating qdo rotating reference frame”.

Stator and Rotor Voltages

$$\begin{aligned}
 v_{qs}^e &= \frac{p}{\omega_b} \psi_{qs}^e + \frac{\omega_e}{\omega_b} \psi_{ds}^e + r_s i_{qs}^e \\
 v_{ds}^e &= \frac{p}{\omega_b} \psi_{ds}^e - \frac{\omega_e}{\omega_b} \psi_{qs}^e + r_s i_{ds}^e \\
 v_{0s} &= \frac{p}{\omega_b} \psi_{0s} + r_s i_{0s} \\
 v_{qr}'^e &= \frac{p}{\omega_b} \psi_{qr}'^e + \left(\frac{\omega_e - \omega_r}{\omega_b} \right) \psi_{dr}'^e + r_r' i_{qr}'^e \\
 v_{dr}'^e &= \frac{p}{\omega_b} \psi_{dr}'^e - \left(\frac{\omega_e - \omega_r}{\omega_b} \right) \psi_{qr}'^e + r_r' i_{dr}'^e \\
 v_{0r}' &= \frac{p}{\omega_b} \psi_{0r}' + r_r' i_{0r}'
 \end{aligned} \tag{2.18}$$

Flux Linkage Equations in Matrix Notification

$$\begin{bmatrix} \psi_{qs}^e \\ \psi_{ds}^e \\ \psi_{0s} \\ \psi_{qr}'^e \\ \psi_{dr}'^e \\ \psi_{0r}' \end{bmatrix} = \begin{bmatrix} x_{ls} + x_m & 0 & 0 & x_m & 0 & 0 \\ 0 & x_{ls} + x_m & 0 & 0 & x_m & 0 \\ 0 & 0 & x_{ls} & 0 & 0 & 0 \\ x_m & 0 & 0 & x_{lr}' + x_m & 0 & 0 \\ 0 & x_m & 0 & 0 & x_{lr}' + x_m & 0 \\ 0 & 0 & 0 & 0 & 0 & x_{lr}' \end{bmatrix} \begin{bmatrix} i_{qs}^e \\ i_{ds}^e \\ i_{0s} \\ i_{qr}'^e \\ i_{dr}'^e \\ i_{0r}' \end{bmatrix} \tag{2.19}$$

Torque Equations

$$\begin{aligned}
 T_{em} &= \frac{3}{2} \frac{P}{2\omega_b} (\psi_{qr}'^e i_{dr}'^e - \psi_{dr}'^e i_{qr}'^e) \text{ N.m} \\
 T_{em} &= \frac{3}{2} \frac{P}{2\omega_b} (\psi_{ds}^e i_{qs}^e - \psi_{qs}^e i_{ds}^e) \\
 T_{em} &= \frac{3}{2} \frac{P}{2\omega_b} x_m (i_{dr}'^e i_{qs}^e - i_{qr}'^e i_{ds}^e)
 \end{aligned} \tag{2.20}$$

It can be noticed that the equations 2.15- 2.20 ,which represent the differential equations for the dynamic simulation for three phase induction machine transformed to stationary and synchronous reference frames, have the term ψ which is simply the multiplication of the flux linkage λ by the rated angular speed ω_b .

$$\psi = \omega_b \lambda \tag{2.21}$$

$$x = \omega_b L \tag{2.22}$$

There are also the superscript s to indicate that the equation is represented in stationary reference frame and the superscript e for the synchronous reference frame.

CHAPTER 3

EXPLANATION OF TWO INDUCTION MOTOR DRIVES VECTOR CONTROL VS. DIRECT TORQUE CONTROL

3.1 Introduction

The field of Variable-Speed-Drive is widely used in industrial applications due to the emergence of high power electronics. Power electronics provides: higher switching speeds, higher V-I ratings and less loss. In addition sense, command and control electronics, via microprocessors, DSP or FPGA's allow less expensive and easier to employ software for system optimization instead of the complex hardware. The most important advantage of all these improvements is that the operating cost is reduced, by electronically reducing the speed when it is not needed instead of lossy gears. One of the old traditional control methods is V/Hertz control, which keeps the ratio of the Volts/Hertz constant in order to keep the flux in the motor constant to provide a wide range of speeds. However, this method controls the magnitude of the voltage only and has a poor dynamic torque response and low speed accuracy especially in low speed motors [3-4], [18]. This old method has been phased out by more effective control methods such as Vector Control and Direct Torque Control, which are explained in this chapter and compared at the conclusion.

When an induction motor is running in steady state, three phase drive can be easily presented as one phase because everything is sinusoidal, balanced and symmetrical. But if the operation requires dynamic changing of motor speed or applying more torque suddenly, the motor voltages and currents are not sinusoidal anymore. The transient response voltages and the currents are shown herein via Vector control and Direct Torque Control to provide a faster response [3].

In this chapter, the concept of dynamic torque in a separately excited dc motor is explained first. This allows us to introduce the concept and principles of the field orientation control methodology. The two most commonly used methods of the vector control are direct vector control and indirect vector control. Herein we explain the concept of Direct Torque Control and the relative stages of methodology for Space Vector Voltage Source Inverter and switching tables. Flux and torque control is presented. Finally, a theoretical comparison between the two methods is presented.

3.2 Vector Control of Induction Motor

It is known that if the flux linkage of the rotor of an induction motor is fixed in special frame, the electromagnetic torque will behave similar to the separately excited DC motor. In the Vector Control method of induction motors, one of the advantages of the separately excited DC motor of being able to decouple the flux control and the torque is thereby opened up. The field orientation control of induction motor allows decoupling the control of magnetic flux and the control of the torque produced by the stator current. This makes the induction motor control more akin to the control of the separately excited DC motor. That is, in three phase induction motor control, the rotor field can be equivalent to the field of excitation of dc motor, but with the difference that the voltage in the rotor, which produces the field, is dependent on the magnetic field in the stator [4].

3.2.1 Torque in separately excited dc motor

By looking to the Fig 3.1 which represents a simple model of separately excited dc motor, the field circuit is shown as two poles pointed as N and S. The armature circuit represented as two brushes which connect the current to the coils in the armature. The field space

vector λ_f is produced by the stator poles which is on the same line with the direct axis. The position of the brushes (armature current flow) which is aligned with the quadrature axis and shifted by the vector of stator field by 90° although the rotor is rotating. It is known that the electromagnetic torque depends on the stator field λ_f and the armature current i_a and the sine the angle between them. Thus the maximum torque can be best achieved if two component, λ_f and i_a , are spatially orthogonal.

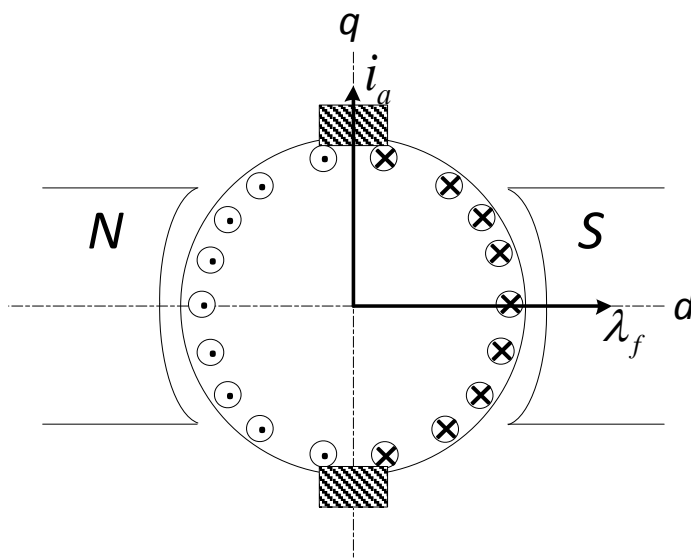


Figure 3.1 Simple representation of separately excited DC motor.

Reproduced without permission from [1].

Due to the fact that λ_f , which is produced by the field current i_f , and the armature current i_a are flowing in different winding, so they can be separately controlled. Generating the optimal torque is not the only advantage of dc motor, but the magnetic field and the torque are controlled separately and that is called decoupling. For the latter reason Vector Control method is known as *decoupling control* and the torque equation which can be used is equation 3.1 [1].

$$T_{em} = k_T \lambda_f i_a \quad (3.1)$$

Where k_T is a constant proportional with the motor's size.

3.2.2 Principles of vector control of Induction motor

Control of a 3-phase squirrel cage induction motor is difficult, because it is not simply about independently controlling the voltage and the frequency only. We show below that Vector control can perform a faster critically damped response that is non-oscillating.

The principle of the vector control is the following: the actual flux value with sine space vector in the air gap, can be presented as a rotating phasor or vector. Hence, the rotor flux linkage Ψ_r is aligned with the direct axis d^e of the of two axes which rotate in the speed of the electromagnetic flux, synchronous speed, ω_e . The other axis of this rotating axes q^e , which is shifted from the perpendicular axis by the angle ρ , which can determine the position with the other two-axis stationary frame ($d^s q^s$). In the synchronous frame, the stator current i_s consists of i_{sq}^e and i_{sd}^e , the term i_{sd}^e is performing the value of I_m and it is affecting the magnitude of Ψ_r . The other component i_{sq}^e which is perpendicular to it, is affecting the electromagnetic torque. Consequently, in this representation the control of the flux and the torque are decoupled. The Fig 3.2 is showing the process [26].

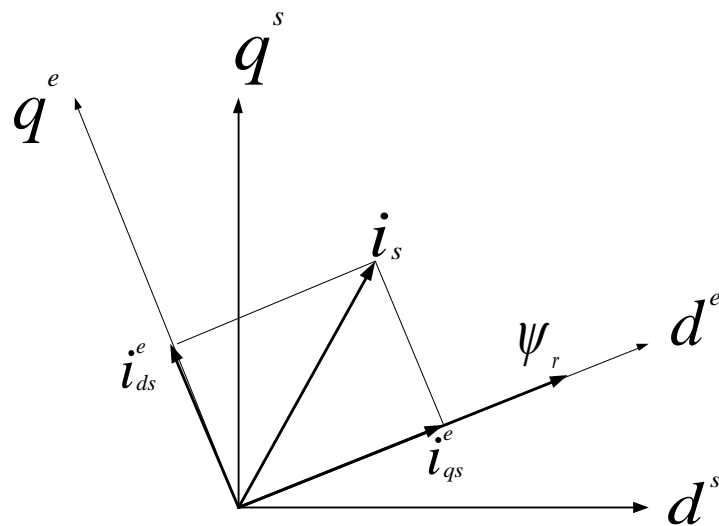


Figure 3.2 Principles of vector control (decoupling between rotor flux and torque)

Unlike the dc motor, the induction motor operating parameters are more difficult to be measured, unless modern Hall Effect flux sensors are employed and information sent to the command and control electronics. The procedure of the control starts with identifying the orientation (the angle) and making a proper selection of the inverter control in order of decoupling i_{sq}^e and i_{sd}^e . This is done in two different ways, measuring the specific flux values or calculating them. These two main methods, which are direct vector control and indirect vector control, are explained in section (section 3.2.4).

The procedure of controlling the induction motor using field orientation involves important mathematical transformations which are summarily explained as follows in three main points:

1. The developed torque and the flux T_{em}^* and λ_f^* should be set and then the corresponding i_{ds}^e and i_{qs}^e in synchronous reference frame are found.
2. Angular position ρ is then found to be used in the transformation from the synchronous reference frame to the stationary frame ($dq^e \rightarrow dq^s$) to achieve desired i_{qs}^s and i_{ds}^s .
3. The last step is to convert the gotten component of stator current in stationary reference frame to the desired three phase currents to be the base of control the inverter [1], [31].

3.2.3 Torque equations for Vector Control

All vector control strategies agree that the machine torque and the flux linkage can be controlled using the stator current vector alone [11]. That is the flux linkage component on the q-axis of synchronous frame, which is featured in the equation 2.19, and equal to zero because the rotor flux is aligned with the d-axis as shown in Fig 3.2.

$$\lambda'_{qr}{}^e = L_m i_{qs}^e + L'_r i'_{qr}{}^e = 0 \quad \text{Wb. Turn} \quad (3.2)$$

$$i'_{qr}{}^e = -\frac{L_m}{L'_r} i_{qs}^e \quad A \quad (3.3)$$

Substituting $\lambda_{qr}^e = 0$ on the torque equation (2.20), the torque equation is simplified to that shown in equation (3.4).

$$T_{em} = -\frac{3P}{2} \lambda'_{dr}{}^e i'_{qr}{}^e \quad N.m \quad (3.4)$$

Substituting the expression of $i'_{qr}{}^e$ which is in equation 3.3 into the resultant torque equation 3.4, the torque will be

$$T_{em} = \frac{3P}{2} \frac{L_m}{L'_r} \lambda'_{dr}{}^e i_{qs}^e \quad (3.5)$$

Therefore, the torque can be controlled using the q-axis component of the stator current alone and the rotor flux linkage is not distressed. Applying the concept of zero q-axis rotor flux linkage, the rotor q-axis voltage can be expressed as:

$$\underbrace{v'_{qr}{}^e}_{=0} = r'_r i'_{qr}{}^e + \underbrace{p \lambda'_{qr}{}^e}_{=0} + (\omega_e - \omega_r) \lambda'_{dr}{}^e \quad V \quad (3.6)$$

If we arrange equation (3.6) as the difference of the two frequencies or the slip frequency

$$(\omega_e - \omega_r) = \frac{r'_r i'_{qr}{}^e}{\lambda'_{dr}{}^e} \quad (3.7)$$

If we assume that $\lambda'_{dr}{}^e$ is constant, the derivative of it becomes zero and applying the previous conditions

$$\underbrace{v'_{dr}{}^e}_{=0} = r'_r i'_{qr}{}^e + \underbrace{p \lambda'_{dr}{}^e}_{=0} - (\omega_e - \omega_r) \underbrace{\lambda'_{qr}{}^e}_{=0} \quad V \quad (3.8)$$

This equation shows that $i'_{dr}{}^e$ has to be zero in order to satisfy the resultant equation of 3.8.

Recalling the equation 2.19 when $i'_{dr}{}^e = 0$, so $\lambda'_{dr}{}^e = L_m i_{ds}^e$ and if we substitute that into equation 3.7 the slip speed will simplify to

$$(\omega_e - \omega_r) = \frac{r'_r i'_{qr}{}^e}{L_m i_{ds}^e} \quad (3.9)$$

Because the rotor flux can be changed by controlling i_{ds}^e , the orientation is accomplished by either keeping the slip speed or the q-axis stator current revolving in synchronous speed based on equation 3.9.

Also, if we take the expression of i_{dr}^e from the equation 2.19 which is $i_{dr}^e = (\lambda_{dr}^e - L_m i_{ds}^e)/L_r'$ and substitute that into the equation 3.8 we get

$$\lambda_{dr}^e = \frac{r_r' L_m}{r_r' + L_r' p} i_{ds}^e \text{ Wb. turn} \quad (3.10)$$

3.2.4 Methods of Vector Control

The way of determining the angle (position) of the rotor flux vector, rotating at the synchronous speed, depends on the type of the field orientation: either *direct field orientation* or *indirect field orientation*

3.2.4.1 Direct Field Orientation Method (DFO)

When the identification of the flux vector is done by direct Hall sensor measurement or even indirectly by estimation of other motor electrical variables, it is called direct field orientation. This method depends on measuring the air gap flux using special sensor is called Hall-Effect-Device. The magnetic flux measured is the mutual flux not the rotor flux, which has angle ρ , which is important to be properly oriented. The connection with the known stator current provides the solution of determining this angle. Proportional Integral (PI) controller methodology is used in both the flux and the torque loops to get the desired direct and quadrature components of the stator current in the synchronous reference frame. Those are then transformed to the same component in the stationary frame. Finally the equations of control are referenced to the three phase motor drive currents to control the inverter operating conditions [1]. The complex multi-step mathematical procedure is explained as follows:

First, the three phases are transformed to d-q stationary components as the equations 3.11 and

3.12

$$i_{qs}^s = \frac{2}{3} i_{as} - \frac{1}{3} i_{bs} - \frac{1}{3} i_{cs} \quad A \quad (3.11)$$

$$i_{ds}^s = \frac{1}{\sqrt{3}} (i_{cs} - i_{bs}) \quad A \quad (3.12)$$

Because $\lambda_{mq}^s = L_m (i_{qs}^s + i_{qr}^s)$, the flux linkage components λ_{qr}^s and λ_{dr}^s can be written as:

$$\lambda_{qr}^s = \frac{L'_r}{L_m} \lambda_{mq}^s - L'_{lr} i_{qs}^s \quad (3.13)$$

$$\lambda_{dr}^s = \frac{L'_r}{L_m} \lambda_{md}^s - L'_{lr} i_{ds}^s \quad (3.14)$$

The calculated λ_{dr}^s and λ_{qr}^s give the ability to obtain the cosine and the sin of the angle ρ using the following equations:

$$\sin\left(\frac{\pi}{2} - \rho\right) = \cos \rho = \frac{\lambda_{dr}^s}{\lambda_{qr}^s} \quad (3.15)$$

$$\cos\left(\frac{\pi}{2} - \rho\right) = \sin \rho = \frac{\lambda_{qr}^s}{\lambda_{dr}^s} \quad (3.16)$$

After determining the angle ρ which is used to the following step, d-q synchronous frame to d-q stationary frame, the transformation will be as follows:

$$i_{qs}^{s*} = i_{qs}^{e*} \cos \rho + i_{ds}^{e*} \sin \rho \quad A \quad (3.17)$$

$$i_{ds}^{s*} = -i_{qs}^{e*} \sin \rho + i_{ds}^{e*} \cos \rho \quad A \quad (3.18)$$

Finally, the stationary reference frame components of stator current are transformed to three phases to control the inverter operating conditions, which set three phase currents and phases to complete the control loop.

$$i_{as}^* = i_{qs}^{s*} \quad A \quad (3.19)$$

$$i_{bs}^* = -\frac{1}{2} i_{qs}^{s*} - \frac{\sqrt{3}}{2} i_{ds}^{s*} \quad A \quad (3.20)$$

$$i_{cs}^* = -\frac{1}{2} i_{qs}^* + \frac{\sqrt{3}}{2} i_{ds}^* A \quad (3.21)$$

This multi-step procedure is shown simplified in the block diagram of the direct field orientation methodology illustrated in Fig 3.3

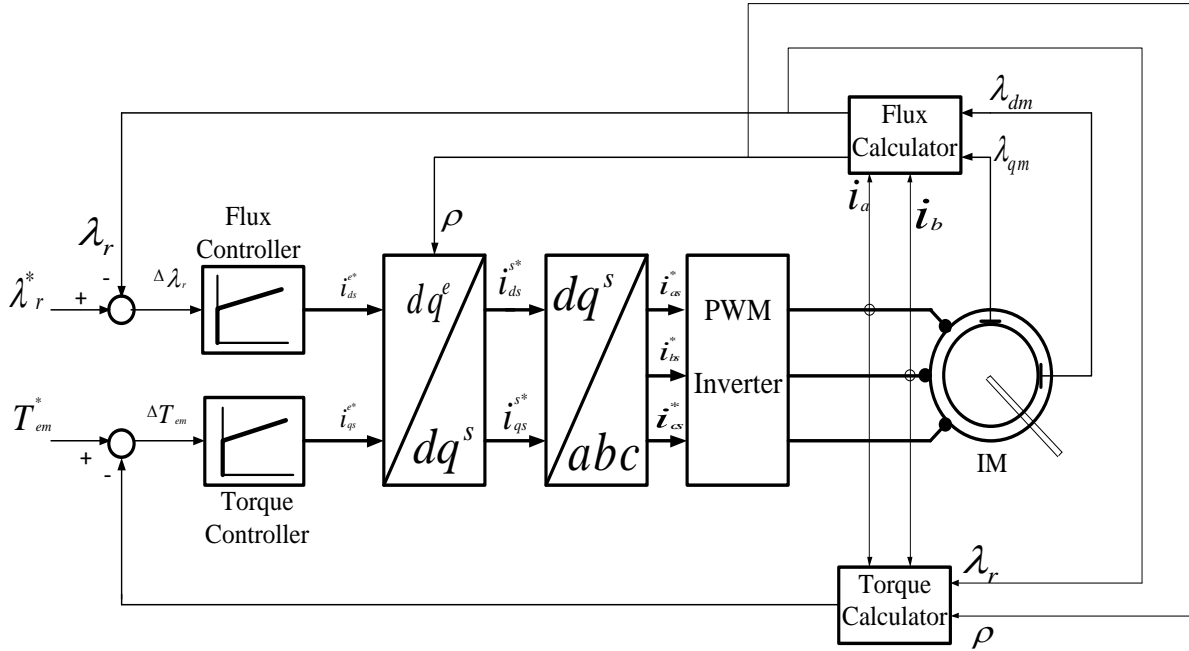


Figure 3.3 The Block diagram of direct vector control of Induction motor.

Practically, this kind of sensor and its position can decrease the degree of ruggedness of the induction motor. In our comparison, this method is going to be used in the comparison with DTC because of the modeling simplicity.

3.2.4.2 Indirect Field Orientation Method (IFO)

The other way of applying vector control methodology to induction motor operation, which is the indirect field orientation (IFO) pathway. This method does not depend on the measurement of air-gap magnetic flux but rather employs equation 3.5 as follows. Torque can be controlled by either changing i_{qs}^e or the slip speed $(\omega_e - \omega_r)$. The rotor flux can also be controlled by varying i_{ds}^e , because if the desired rotor flux is measured or given, then the i_{ds}^{e*} is determined by using equation 3.10. Then, the desired torque can be found as equation 3.22.

$$T_{em}^* = \frac{3P}{2} \frac{L_m}{L_r'} \lambda_{dr}^{e*} i_{qs}^{e*} \quad (3.22)$$

Equation 3.9 has shown that the optimum orientation of i_{dr}^{e*} is to be zero, so the desired slip speed is as summarized equation (3.23).

$$\omega_2^* = (\omega_e - \omega_r) = \frac{r_r' i_{qr}^{e*}}{L_m i_{ds}^{e*}} \quad (3.23)$$

Fig 3.4 shows the block diagram of the indirect torque control of an induction motor. Notice that the angle of orientation (ρ) is the summation of the rotor angle (θ_r) and the slip speed angle (θ_2). If the values of the cosine and the sin of the rotor angle are known by the magnetic sensor, the orientation angle can be determined using the equations 3.24 and 3.25, the simple trigonometry relations.

$$\cos \rho = \cos(\theta_r + \theta_2) = \cos \theta_r \cos \theta_2 - \sin \theta_r \sin \theta_2 \quad (3.24)$$

$$\sin \rho = \sin(\theta_r + \theta_2) = \sin \theta_r \cos \theta_2 + \cos \theta_r \sin \theta_2 \quad (3.25)$$

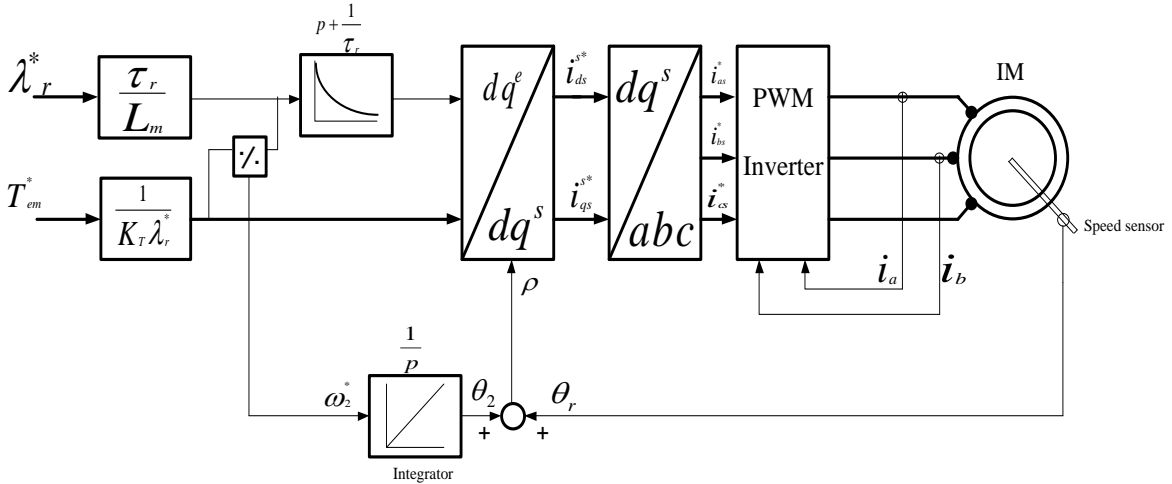


Figure 3.4 Block diagram of indirect vector control of Induction motor.

3.3 Direct Torque Control

With vector control method for induction motor operation, the magnitude and the phase of stator voltage can be controlled. Direct torque control has a very fast response and simple

structure which makes it to be more popular used in industrial world. This method of control implies a comparative control of the torque and the stator fluxes which must fall into two separate certain bands (limits) to be applicable [3], [16].

3.3.1 The Basic Principles of Direct Torque Control of Induction Motor

The basic concept of the Direct Torque Control (DTC) method was proposed by Takahashi and Noguchi in 1986. This method is more used in controlling the induction motor because it is considered a simple and robust method. The power inverter operational control is an important key in this method and modern power electronics has made this cost effective as well. The simple objective is to control two quantities which are the stator flux vector and the electromagnetic torque. Those quantities are directly controlled by selecting the proper inverter state with a combination of sense, command and control feedback loops and by power electronics drive control in the inverter stage. High dynamic performance can be achieved by the stator flux because the latter is close to being sinusoidal.

The stator EMF depends on the stator flux, so the magnitude of the EMF depends on the stator voltage. Hence, $\lambda_s = \int (V_s - r_s i_s) dt$, and the torque, as the general definition, is the cross product of the stator flux and the rotor flux. As a result, the magnitude of the stator flux and the developed electromagnetic torque can be adjusted by selecting the state of the inverter of space vectors of the stator voltage [1],[26].

3.3.2 Space Vector Modulation of Three Phase Voltage Source Inverter with DTC

If the voltage vector is shifted (lag or lead) with respect to the stator flux vector by an angle which is not more than 90° , this causes the flux to increase and vice versa. The developed torque is then directly controlled by selecting the inverter situation in order to boost the stator

flux up or buck it down. The circuit diagram of the inverter is shown in Fig 3.5 and the state of square-wave operation as in Fig 3.6; the voltage vector is obtained by the equation 3.26.

$$V_K = V_i e^{j\theta_{v,K}} \quad (3.26)$$

When V_i is the dc voltage rare, and $\theta_{v,K}$ is given as:

$$\theta_{v,K} = (K - 1) \frac{\pi}{3} \quad (3.27)$$

The plane is divided by 6 sectors; hence each sector has a 60° interval as shown in Fig3.7. K, in Equations (3.26) and (3.27), is the sector number which defines the state of the inverter. Because the stator flux vector, which can be defined as $\lambda_s = |\lambda_s| e^{j\theta_s}$, is depending on the complex stator voltage (V_K), when the voltage falls into the a specific sector K that means the operation is on that sector.

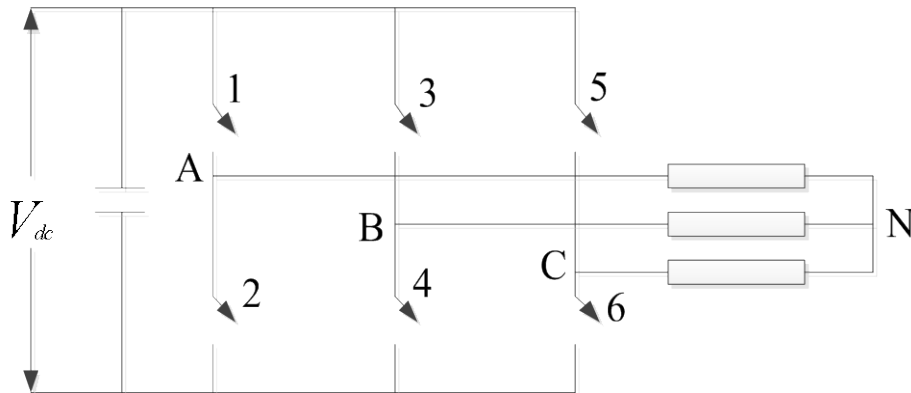


Figure 3.5 Circuit Diagram of Three phase Voltage Source Inverter, where control of the switch sequencing allows determination of the frequency and the phase of the generated AC.

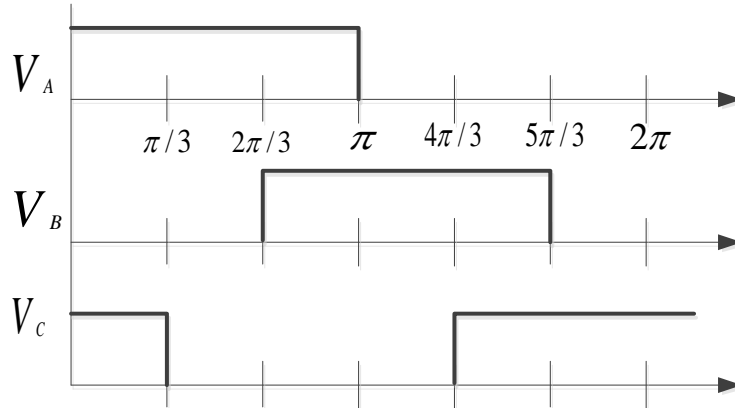


Figure 3.6 Three phase square-wave forms which is produced by the inverter in Fig 3.5.

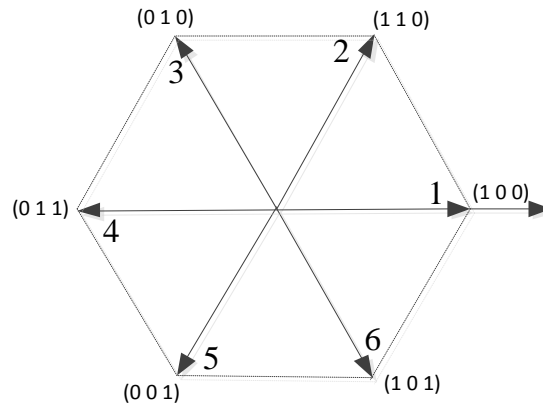


Figure 3.7 Illustrative Phase Voltages in Space Vector

3.3.3 Basic principles of Switching Table

The main concept for employing a switching table in DTC is that the measured values of stator flux and electromagnetic torque are compared to reference values, i.e. λ_s^* and T_{em}^* through what is called hysteresis controller. These two hysteresis controllers are different for Torque and flux. Because the flux and torque have to fall into a certain band for switching table DTC, we have two limits, which is considered as the tolerance number of allowing being “how far” from the desired value we can employ this method and still be accurate. In practice, the flux controller provides two cases (a two level controller). In contrast to achieve the desired output torque the hysteretic controller need provide three separate cases. The equations 3.28 and 3.29 represent the

hysteresis band limits for the flux tables and equations 3.30 through 3.32 represent the three levels hysteresis bands of the torque tables [16].

$$\lambda_{err} = 1, \text{ for } \lambda_s < \lambda_s^* - \varepsilon_\lambda \quad (3.28)$$

$$\lambda_{err} = -1, \text{ for } \lambda_s < \lambda_s^* + \varepsilon_\lambda \quad (3.29)$$

$$T_{err} = 1, \text{ for } T_{em} < T_{em}^* - \varepsilon_T \quad (3.30)$$

$$T_{err} = 0, \text{ for } T_{em} = T_{em}^* \quad (3.31)$$

$$T_{err} = -1, \text{ for } T_{em} < T_{em}^* + \varepsilon_T \quad (3.32)$$

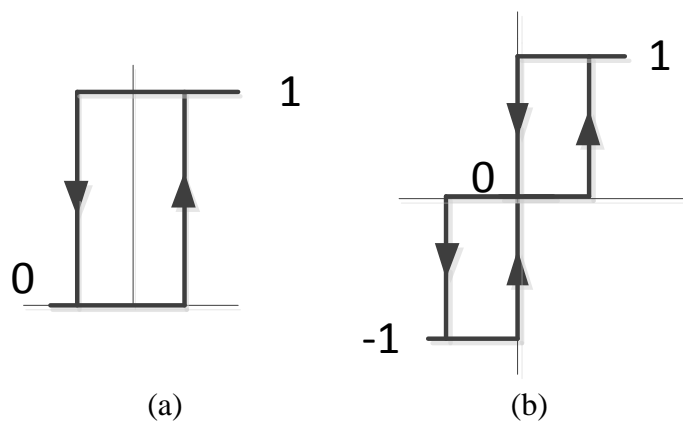


Figure 3.8 Hysteresis bands
 (a) the stator flux, (b): electromagnetic torque

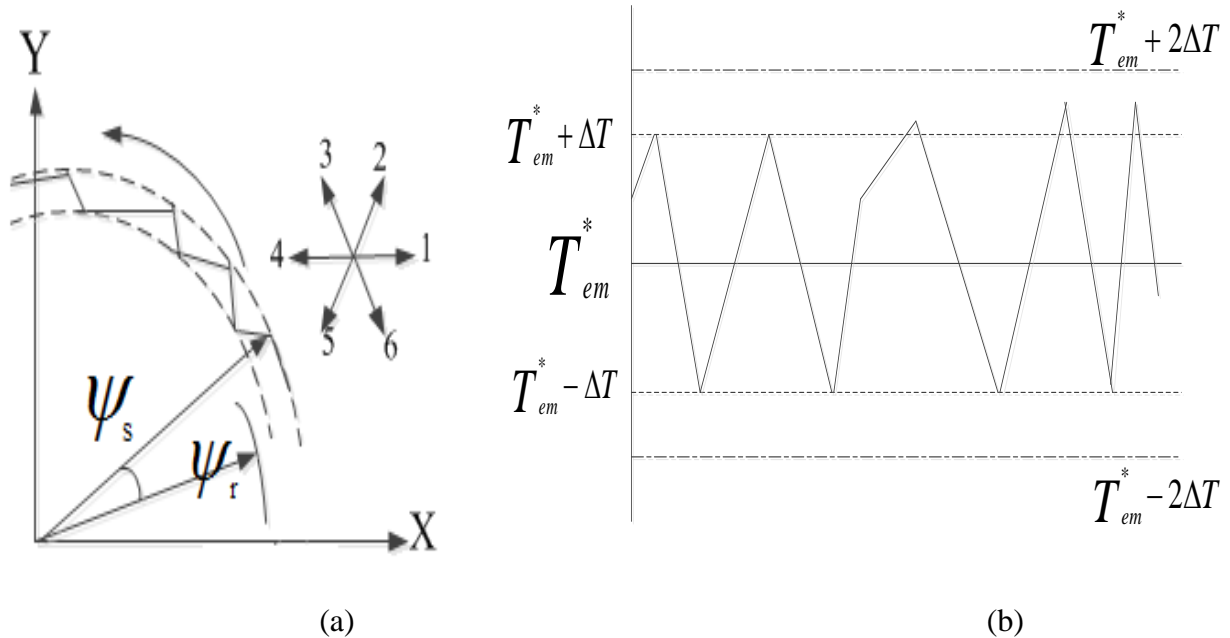


Figure 3.9 (a): The hysteresis band controls the stator flux voltage, (b): The torque is controlled by the three level hysteresis bands.

Reproduced without permission from [23]

Table3. 1 The effect of the voltage vector on the stator flux vector in Sector I

\vec{v}_s	T_{em}	λ_s^{\wedge}
\vec{v}_3	Increase	Increase
\vec{v}_2	Increase	Decrease
\vec{v}_4	Decrease	Decrease
\vec{v}_5	Decrease	Increase

Where $2\varepsilon_\lambda$ is the flux tolerance band and $2\varepsilon_T$ is the torque tolerance band. Table 3.1 represents the switching table logic based on the equations 3.28 to 3.32. This results in the six sectors of the hysteretic table below for inverter outputs.

Table 3.2 Switching table of inverter vector voltages

$ \lambda_{err} $	T_{err}	Sectors					
		I	II	III	IV	V	VI
FU	TU	V ₂	V ₃	V ₄	V ₅	V ₆	V ₁
FU	TD	V ₆	V ₁	V ₂	V ₃	V ₄	V ₅
FD	TN	V ₇	V ₀	V ₇	V ₀	V ₇	V ₀
FD	TU	V ₃	V ₄	V ₅	V ₆	V ₁	V ₂
FD	TD	V ₅	V ₆	V ₁	V ₂	V ₃	V ₄
FD	TN	V ₀	V ₇	V ₀	V ₇	V ₀	V ₇

It should be noted that FU: Flux Up, TU: Torque Up, FD: Flux Down, TD: Torque Down and TN: Torque Neutral. The voltages from V₁ to V₆ are the active voltage vectors and V₀ and V₇ are the zero voltages.

3.3.4 Stator Flux Linkage and Torque Control

When the proper inverter voltage sequence (V₁-V₆) is selected, the stator flux is going to be rotating at the desired synchronous speed within the specified band. As mentioned earlier, the stator flux monotonically follows the stator voltage, when the stator resistance is small enough to be neglected. Thus, changing the stator flux space vector can be accomplished by changing the stator voltage during a desired period of time.

$$V_s = \frac{d\psi_s}{dt} \rightarrow d\psi_s = V_s dt \quad (3.33)$$

$$\text{i.e.} \quad \Delta\psi_s = V_s \Delta t \quad (3.34)$$

We can obtain the electromagnetic flux using equation 3.8 and the electromagnetic torque depends on the sin of the angle between the stator flux and rotor flux, i.e. θ_{sr} , as $\theta_{sr} = \theta_s - \theta_r$. Since it is easier to adjust the stator flux through the stator voltage, the variation of the developed electromagnetic torque is done by varying the stator flux vector, the stator flux magnitude and the angle between stator flux and rotor flux as equation 3.9. It is summarized in Fig 3.9 that is Direct Torque Control Block Diagram of Induction motor operation.

$$T_{em} = \frac{3}{2} \frac{P}{2} \frac{L_m}{L'_s} \psi_s \psi_r \sin \Theta_{sr} \quad (3.34)$$

$$\Delta T_{em} = \frac{3}{2} \frac{P}{2} \frac{L_m}{L'_s} (\psi_s + \Delta \psi_s) \psi_r \sin \Delta \Theta_{sr} \quad (3.35)$$

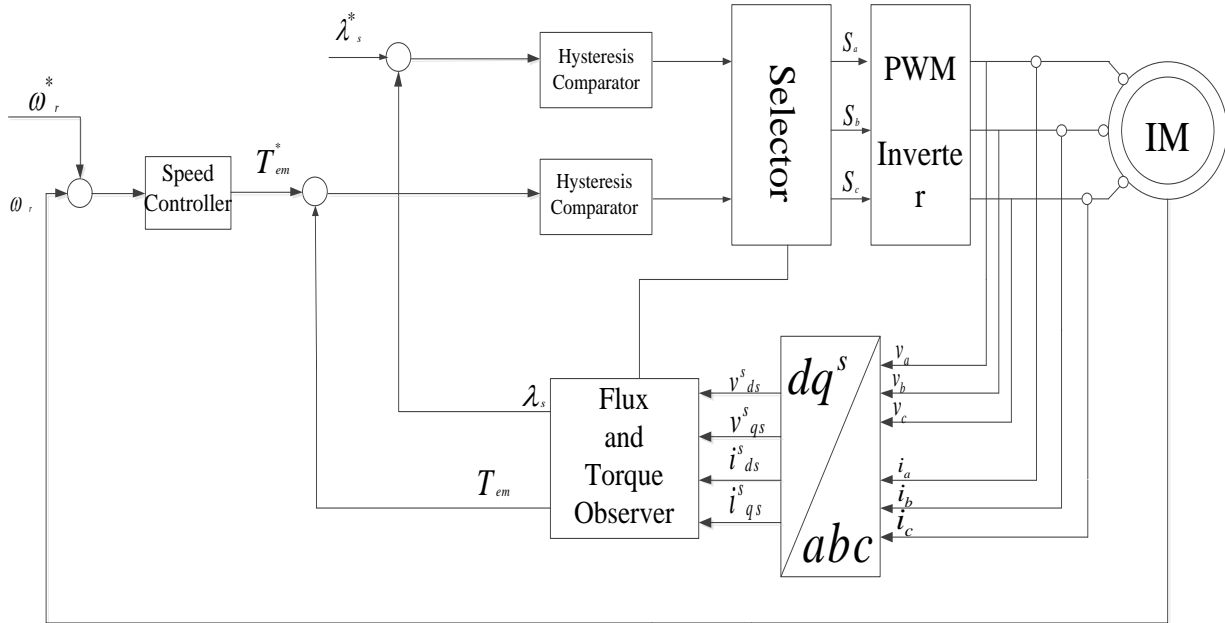


Figure 3.10 Block diagram of the Direct Torque Control of Induction motor

3.4 Theoretical Comparison Vector Control and Direct Torque Control

- The field orientation of vector control method depends on the rotor time constant $\tau_r = L_r / r_r$, and it is known that the rotor resistance can be changing by the effect of the rotor temperature changing and the inductance also changes due to magnetic core flux saturation level.
- DTC is simpler and easier than FOC in practical and software implementations. Because of this, DTC is gaining more popularity in the industrial world.
- In Vector control, the encoder (speed sensor) is always required. DTC, in contrast does not require the encoder unless to get higher accuracy.

- Vector control has a slower flux dynamic control response whereas DTC has faster flux dynamic response.
- Vector control allows less torque ripple on mechanical loads than DTC.

The last theoretical comparisons are based on theoretical studies in the past [17]. A simulation comparison is done in details in Chapter 4. The comparison is conducted based upon some important aspects such as the torque response, speed, flux response and others. Power quality issues are going to be considered in chapter 4 which are voltage sag and short interruptions.

CHAPTER 4

SIMULATION, RESULTS AND DISCUSSION

4.1 Introduction

Recently, the high performance control of induction motors has been interesting to the researchers in industry, because the induction motor is the most commonly used machine and it advances in power electronics have made possible new control methods. Dynamic numerical simulation is very important to decide whether the new control design processes are valid and to avoid the mistakes early in simulations before actual real implementation. MATLAB/ SIMULINK has been a very powerful tool to model the electrical and the mechanical systems because of its simplicity. In this chapter, the dynamic simulation of induction motor is first performed employing the MATLAB/ SIMULINK. Vector control methods and Direct Torque Control method on induction motors follows. A comparison between those two methods is accomplished based upon many aspects but with emphasis on the speed response, torque response, and others detailed herein. The comparison aspect I focus on is the sensitivity of those driving methods to the voltage sag and short circuit interruption, where to my knowledge no prior work has been published. Herein I consider power quality issues and test those two techniques under those two fault conditions.

4.2 Mathematical model simulation using MATLAB/ SIMULINK

Earlier in the thesis, the induction motor mathematical representation was explained. The electrical equations relating the motor voltages, current and flux linkages were given. The mechanical equations of the torque, speed are also found in chapter 2.

It is known that the inductances of the induction motor are changing with time, so the induction motor is now modeled and using the d-q arbitrary frame transformations (Stationary

and/or Synchronous). Modeling the induction motor using those transformations is also convenient, when there is an unbalanced voltage and other parameters variance and gives the opportunity to observe any variable of the motor variables [7],[25].

4.2.1 Three phase to d-q stationary reference frame

Referring to the equation 3.12 in chapter 2, the stationary transformation matrix will be employed as in equation 4.1. This is done by substituting $\theta = 0$ and that is obvious because the stationary frame does not move. It is noticed that some references and books call this transformation (abc to $\alpha\beta$).

$$\begin{bmatrix} v_{ds}^s \\ v_{qs}^s \end{bmatrix} = \begin{bmatrix} \frac{2}{3} & -\frac{1}{2} & -\frac{1}{2} \\ 0 & -1/\sqrt{3} & 1/\sqrt{3} \end{bmatrix} \begin{bmatrix} v_{as} \\ v_{bs} \\ v_{cs} \end{bmatrix} \quad (4.1)$$

That is modeled using SIMULINK as Fig. 4.1 by entering the three phase voltages to the Mux and then applying the mathematical operations using the Function Block Parameters *Fcn*.

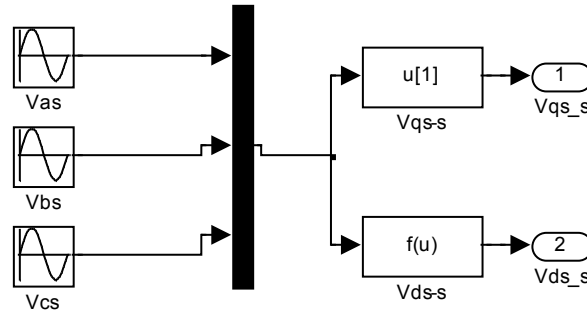


Figure 4.1 Three phase to d-q stationary frame transformation

4.2.2 d-q stationary frame to d-q synchronous frame

The synchronous frame, as mentioned in chapter 2, is the frame which rotates in the speed of electric field in the air gap (synchronous frame). The transformation is done using

equations 4.2 (a) and (b) and uses that in the SIMULINK model to get Fig 4.2. Repeating sequence block is representing θ_e to make this frame rotate in synchronous speed ω_e .

$$v_{qs}^e = v_{qs}^s \cos \theta_e - v_{ds}^s \sin \theta_e \quad (4.2.a)$$

$$v_{ds}^e = v_{qs}^s \sin \theta_e + v_{ds}^s \cos \theta_e \quad (4.2.b)$$

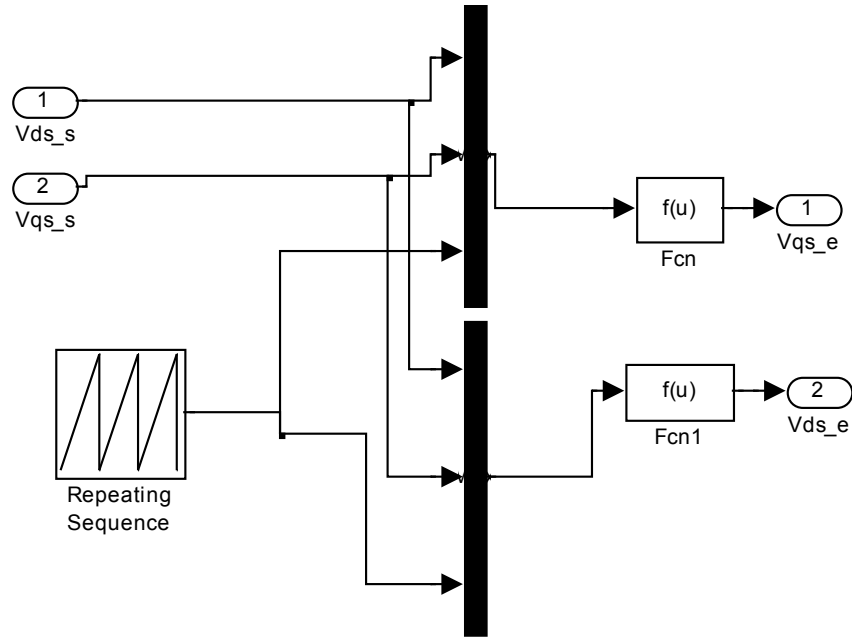


Figure 4.2 Transformation from d-q stationary frame to d-q synchronous frame

4.2.3 Electromagnetic Torque Equation modeling

Simply, referring to the equation 2.17 and we make those simple mathematical operations to get the electromagnetic torque.

$$T_{em} = \frac{3 P L_m}{4} (i_{dr}^s i_{qs}^s - i_{qr}^s i_{ds}^s)$$

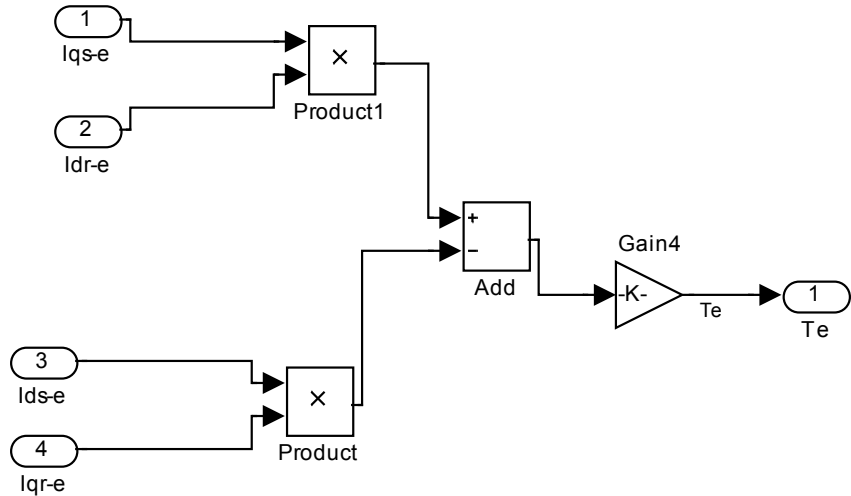


Figure 4.3 Electromagnetic Torque based upon the equation 2.17

The electromagnetic torque and the speed equation is expressed as the equation 4.3 and 4.4 respectively.

$$T_{em} = T_L + B\omega + J \frac{d\omega}{dt} \quad (4.3)$$

$$\omega_0 = \int_{\tau=0}^t \frac{(T_{em} - T_L - B\omega)}{J} d\tau \quad (4.4)$$

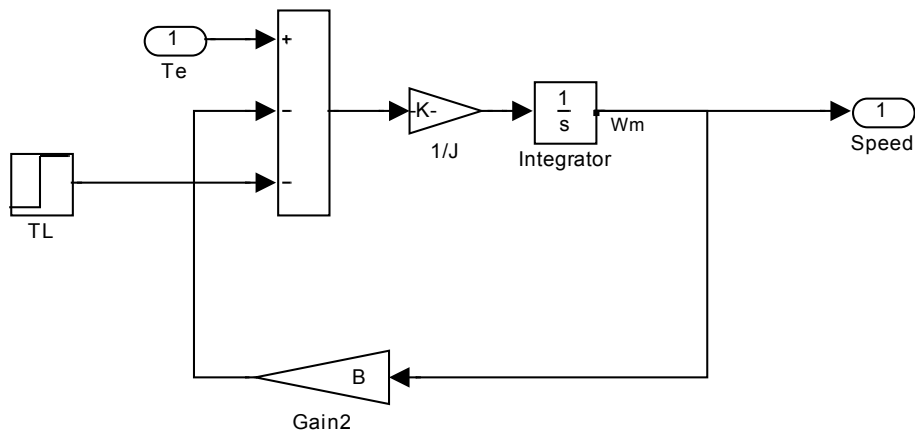


Figure 4.4 The mechanical output of the induction motor Model (Torque and speed)

When we combine the subsystems in Fig 4.1 to 4.4, we get the complete SIMULINK model of three phase induction motor which is shown in Fig 4.5. This chosen model is employed to compare and contrast the two driving methods studied in this thesis project. In the following

sections 4.3 and 4.4, the Direct Field Orientation Control (DFOC) method and Direct Torque Control (DTC) method are explained respectively.

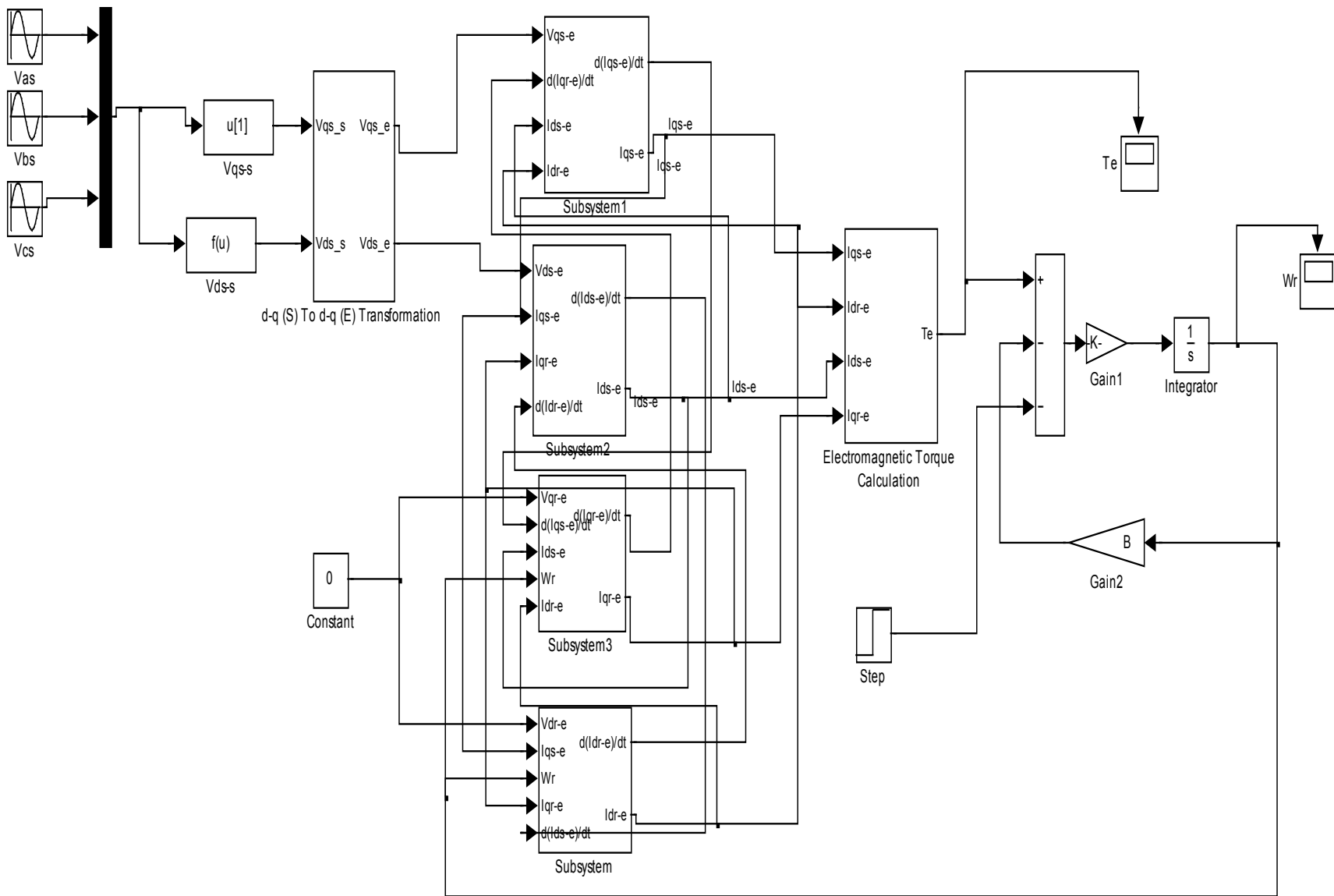


Figure 4.5 Complete SIMULINK model of three phase Induction Motor

4.3 Field Orientation Control (FOC) using MATLAB/ SIMULINK

Referring to the Fig 3.3 and section 3.2.4.1, which show the step by step of Vector Control method, we simulate that using MATLAB/SIMULINK as the following steps:

The proportional Integral controller (PI) is used to obtain the reference synchronous quadrature axis component of the stator current i_{qs}^{e*} . The other component i_{ds}^{e*} is obtained based upon the equation 4.5, which is also used earlier to obtain equation 3.9, and that is done by assuming that λ_{dr}^{e} is constant. The model to perform that is shown in Fig 4.6.

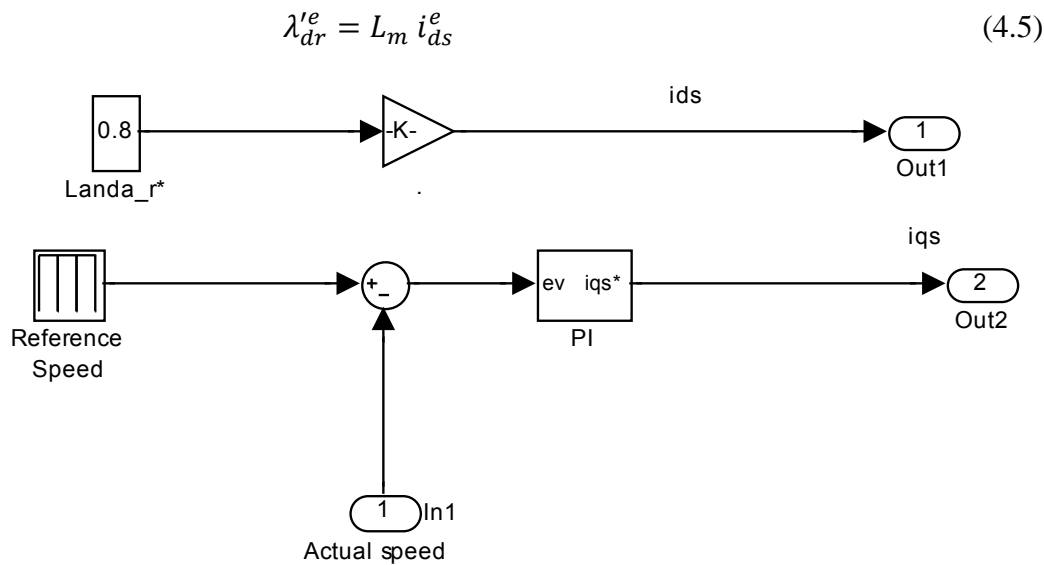


Figure 4.6 obtaining the reference i_{ds}^{e*} and i_{qs}^{e*} through the rotor flux and the speed error.

The obtained i_{ds}^{e*} and i_{qs}^{e*} are then transformed to the same components in the stationary reference frame to be i_{ds}^{s*} and i_{qs}^{s*} . This transformation uses the angular position " ρ ". This transformation is the inverse transformation which is presented in Fig 4.2 but using other angle ρ . That is presented in chapter 3 in the equations (3.17) and (3.18) and that is represented in Fig 4.7.

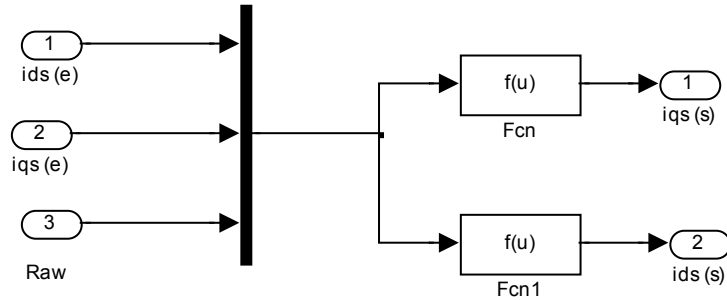


Figure 4.7 transforming the two components of stator current from synchronous reference frame to stationary reference frame.

The last step is to transform those two components of stator current in stationary reference frame based upon equations 3.19 to 3.21 and then have the reference three phases of the stator current and compare it with the actual three phases current to control the PWM inverter. This transformer is shown in Fig 4.8.

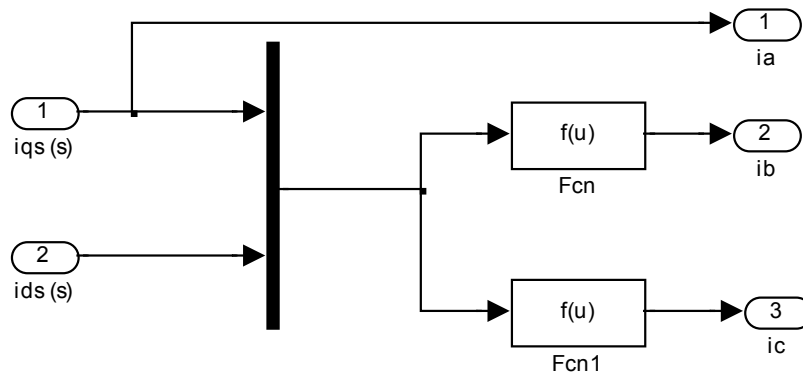


Figure 4.8 d-q stationary reference frame to the reference three phase currents.

Clearly the three phases current are controlling the PWM inverter. The latter is then generating the three phase voltages to be connected to the model of induction motor, which was explained earlier in the section 4.2. The complete model of the Direct Field Orientation is shown in Appendix B.

4.4 Direct Torque Control (DTC) using MATLAB/ SIMULINK

Based upon the section 3.3, the DTC technique starts with setting a reference (desired) torque and reference stator flux. Those two are then compared with the actual instantaneous

torque and stator flux. The difference between the actual and the desired, the error, is controlling the situation, which is the torque. Magnetic stator flux has to be according to the equations 3.28 through 3.32 and illustrated in Fig 3.8. Those two errors are then inputted to two different hysteresis controllers to be inputted to the Interpreted MATLAB Function block with the stator angle. The hysteresis controllers can be represented using the Relay function block. The steps are shown in Fig 4.9.

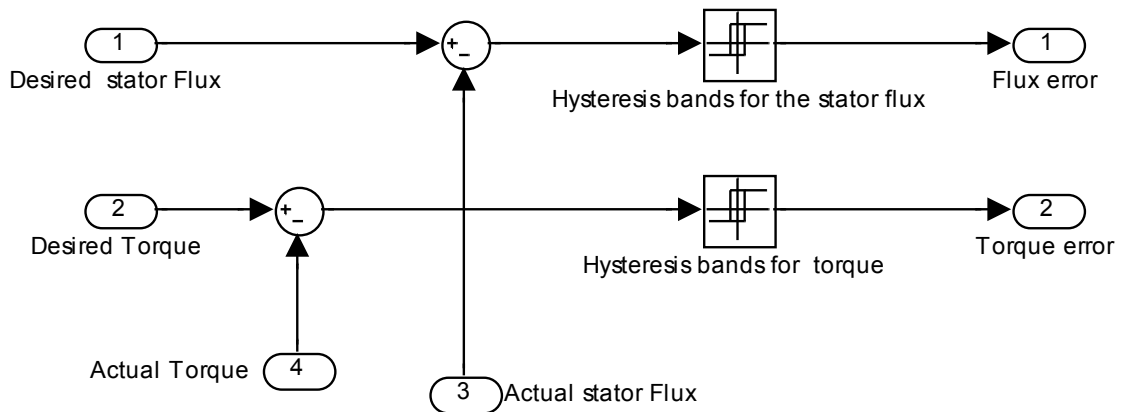


Figure 4.9 The function of the Hysteresis controllers using Relays.

The special Function block which is called “Interpreted MATLAB Function” and that is connected to the “.M” file which is coded to do the function of the switching table which is explained in section 3.3 to generate the PWM three phase voltages to feed the induction motor model. The actual outputs of the motor (Driven) this time are the speed, electromagnetic torque, and flux are gotten. Some of the latters are compared with the desired values for those as a feedback. The code of the switching table logic is presented in Appendix C.

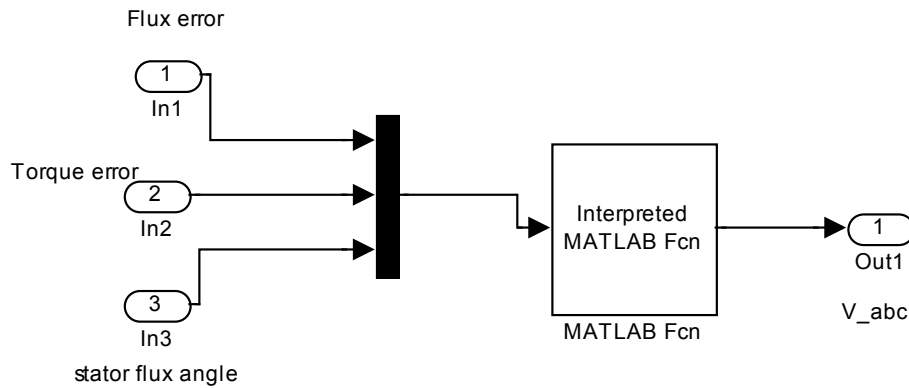


Figure 4.10 Interpreted MATLAB Fcn is representing the switch table logic

The complete Simulink model of the Direct Torque Control is shown in Appendix D, as it is more detailed than necessary at this stage. Although the simulation based comparison has not started yet, we can notice one very clear advantage of the DTC over the FOC is that the DTC is easier to implement numerically and conceptually less complicated. One of the reasons of that advantage is that the DTC doesn't have to have the transformations from the d-q synchronous frame to d-q stationary frame for decoupling control. The next section presents the waveforms of the outputs for the two driving to compare between them in two situations. The first situation is the normal operation and the other situation is when we have voltage sag or short interruption and determining that which technique of those two is more sensitive to this phenomenon. The motivation of the comparison under this kind of power quality issue is that the driving systems are sensitive to these kinds of faults and no published comparison has taken this aspect into consideration between those two particular techniques.

4.5 Simulation Results

The results which are presented and compared are the torque, speed, stator flux and the three phase current of the stator.

4.5.1 Simulation Results in the normal operation case

As mentioned before and based on the simulation, the DTC modeling is easier to achieve than the FOC. In this section, speed, electromagnetic torque, stator flux and the three phase current are going to be compared in the normal operation. After the simulation is done, the following results are extracted. The reference speed was set as shown in Fig 4.11 in both models and the flux was set to 0.8 Wb. The motor is loaded at the 4th second by 7 N.m i.e. fully loaded.

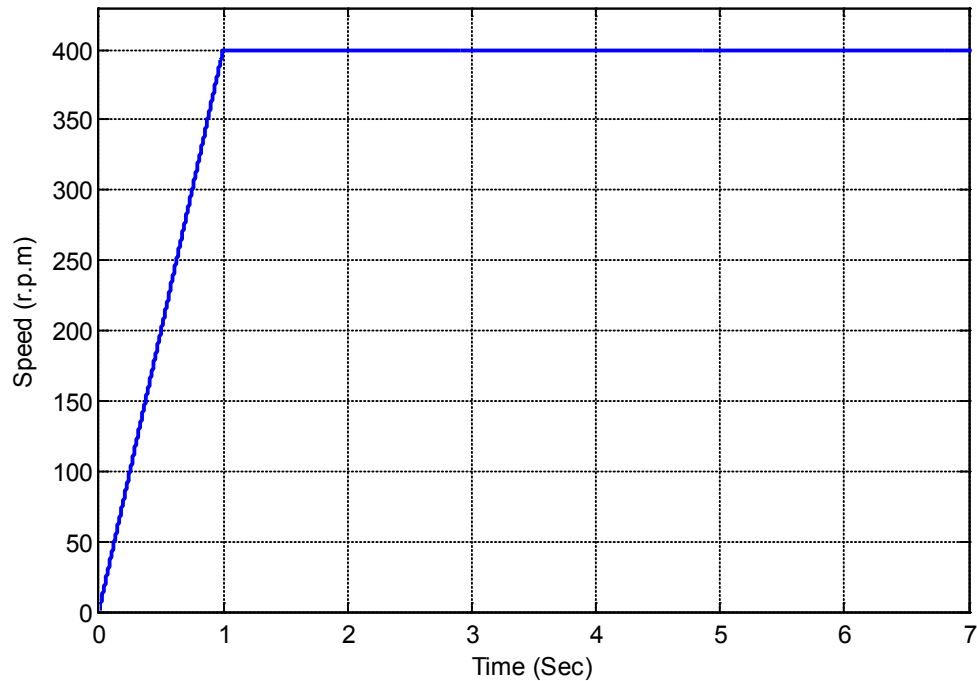


Figure 4.11 Reference motor Speed (rpm) Vs. Time (sec)

4.5.1.1 Speed Comparison

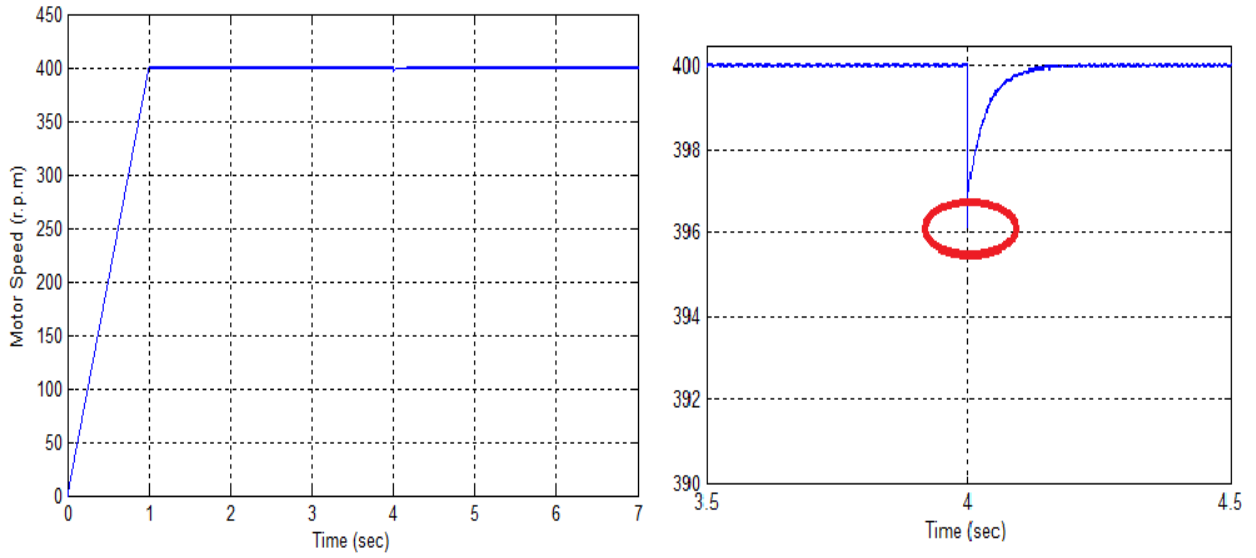
By looking to Fig 4.12, we can notice that the speed for both models is following the desired path until the motor is step torque loaded in the 4th second. When the motor is loaded, we can notice that the deviation of the speed due to the load is so small in Field Orientation Control (FOC) and the speed returns to the desired speed in 0.15 second and the deviation of the speed reaches 396 rpm as shown in (a). In (b), the speed decreases till 117 rpm and returns to the desired speed after 1 sec. That shows the advantage of FOC over DTC in speed response.

4.5.1.2 Torque Comparison

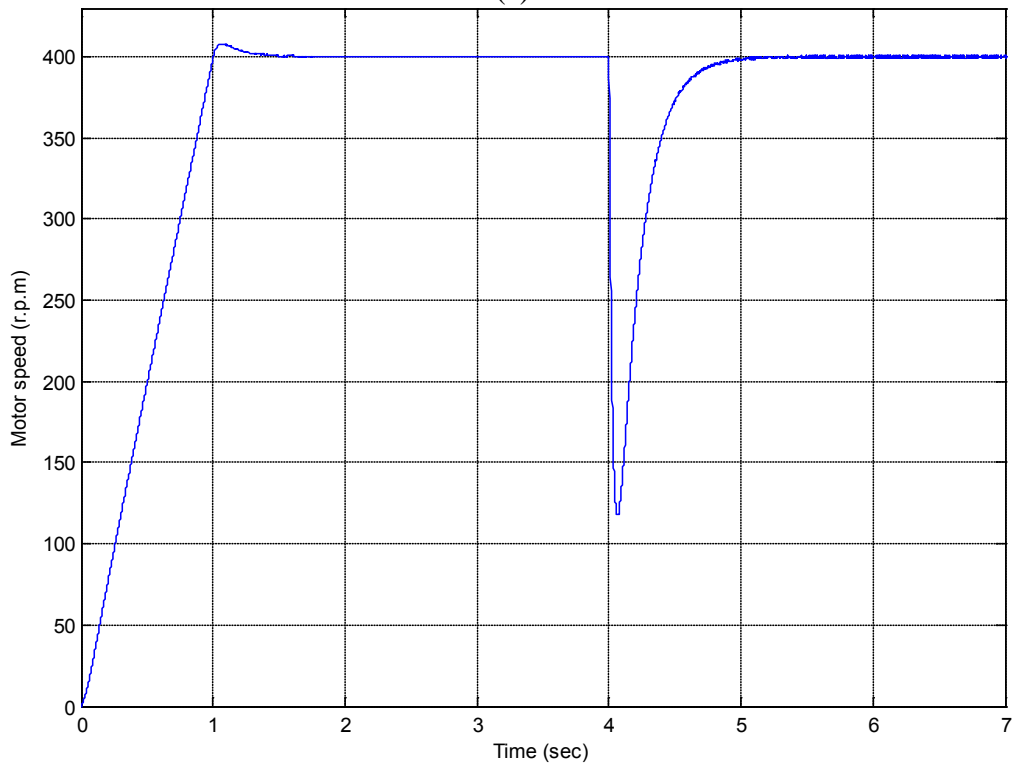
If we look at the resultant torque for both models which are shown in Fig 4.13, we can say that the torque in (a), which is FOC model has less transient ripples. The torque in (b), which is the DTC model, is smoothly following the load torque and it reaches the desired torque slower, but in (a) we can see the spike in the torque when the motor is suddenly loaded (it reaches 8.5 N.m). The bad effect of that spiky torque is that the motor is forced to draw a higher current especially, when we have load torque which has to be applied for certain time and then switched off and so on and if the motor is overloaded (even for short time) the situation becomes more dangerous and the protection system may work to disconnect the unit.

4.5.1.3 Stator Flux Comparison

The stator flux response as it is shown in Fig 4.14, it is quite is different in (a) and (b). First, the stator flux response is much faster in DTC case (b) whereas it reaches the desired value “0.8 Wb in 6.5 msec. In (a), the stator flux becomes as the desired flux in 0.5 sec.



(a)



(b)

Figure 4.12 Motor speed response (a) FOC (b) DTC.

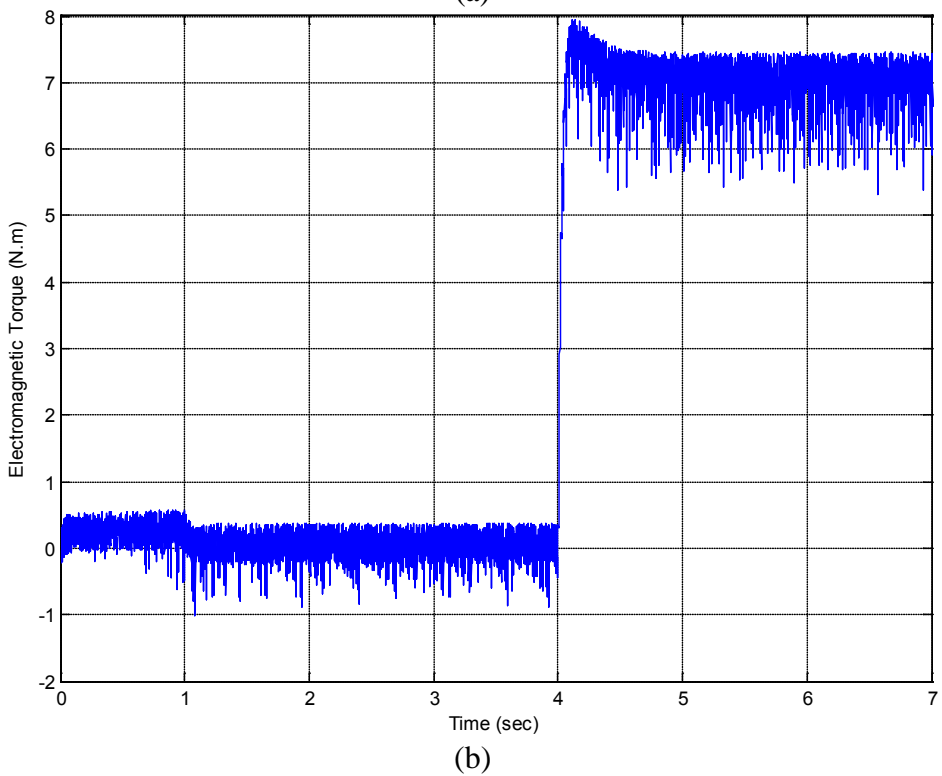
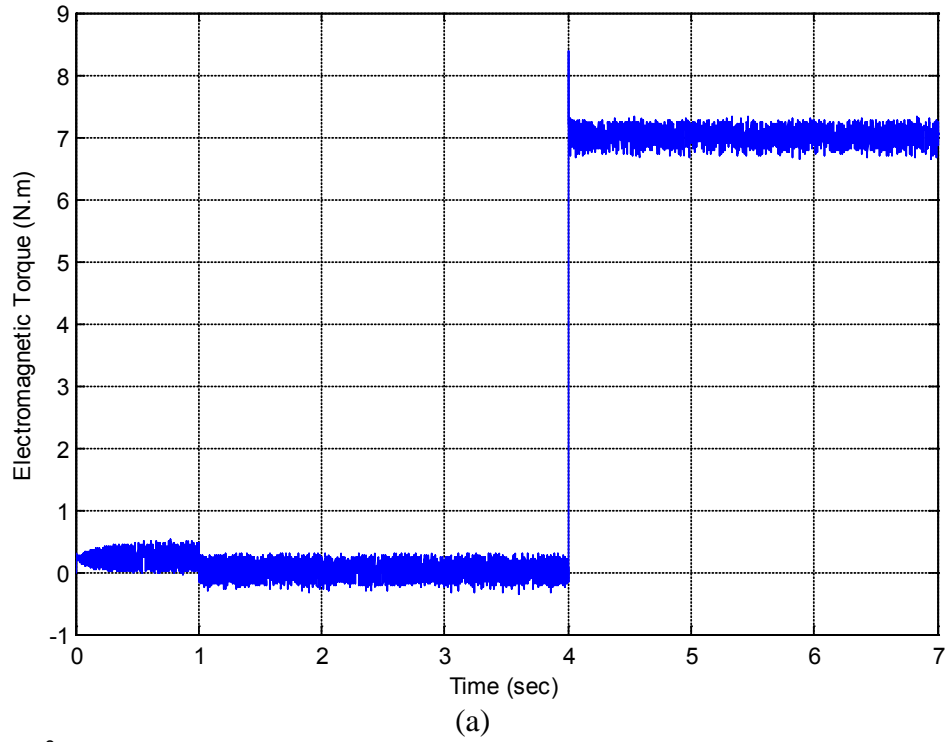
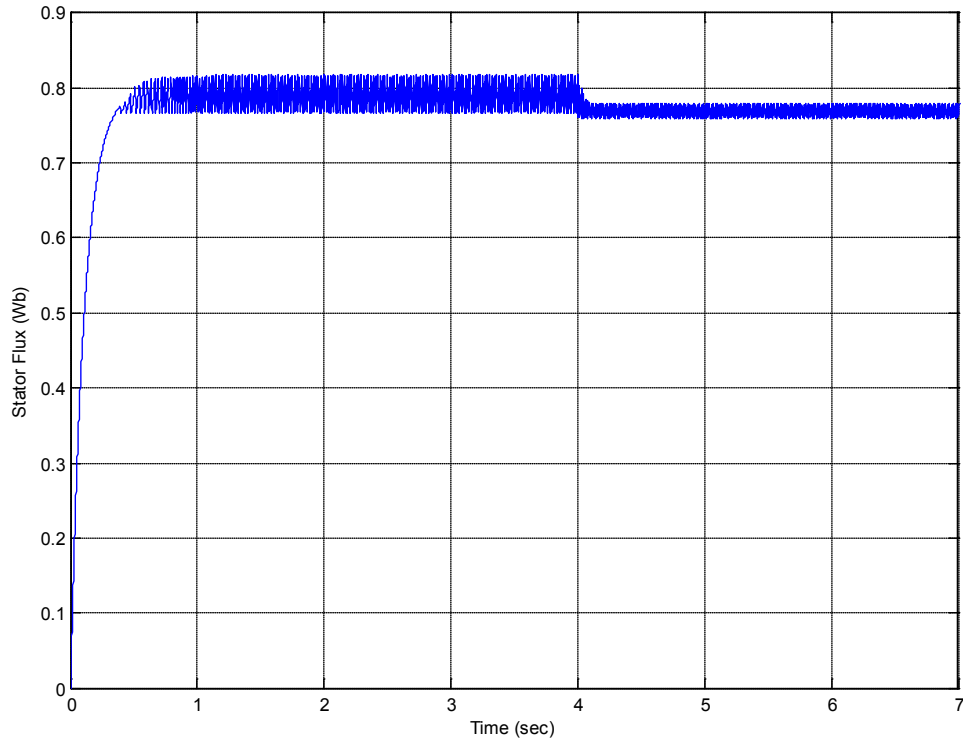
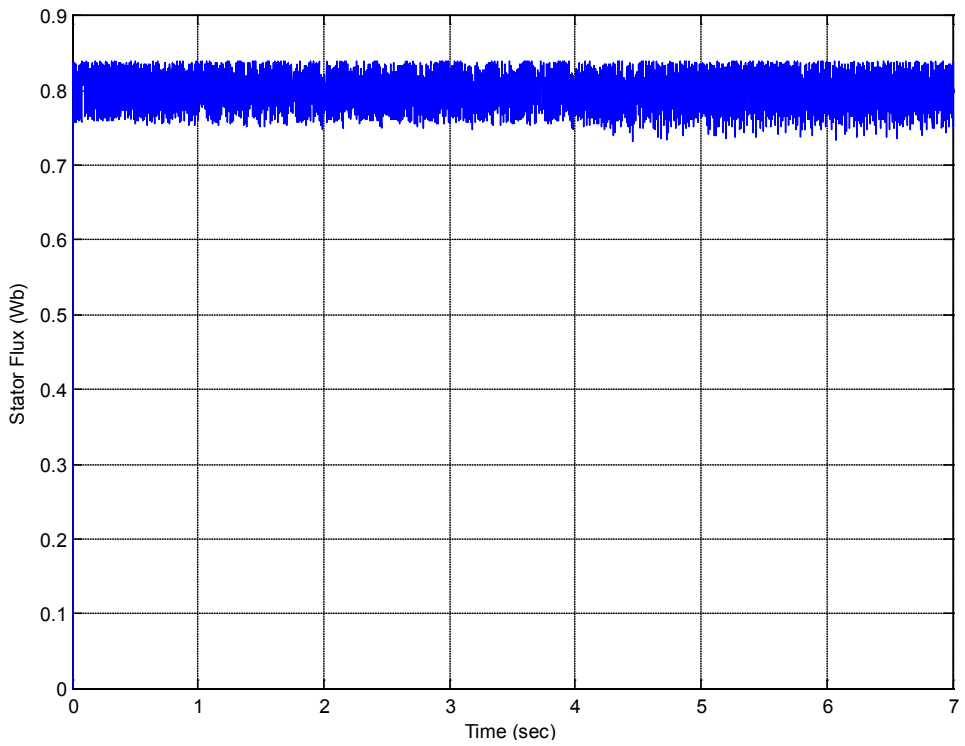


Figure 4.13 Electromagnetic Torque (a) FOC (b) DTC



(a)



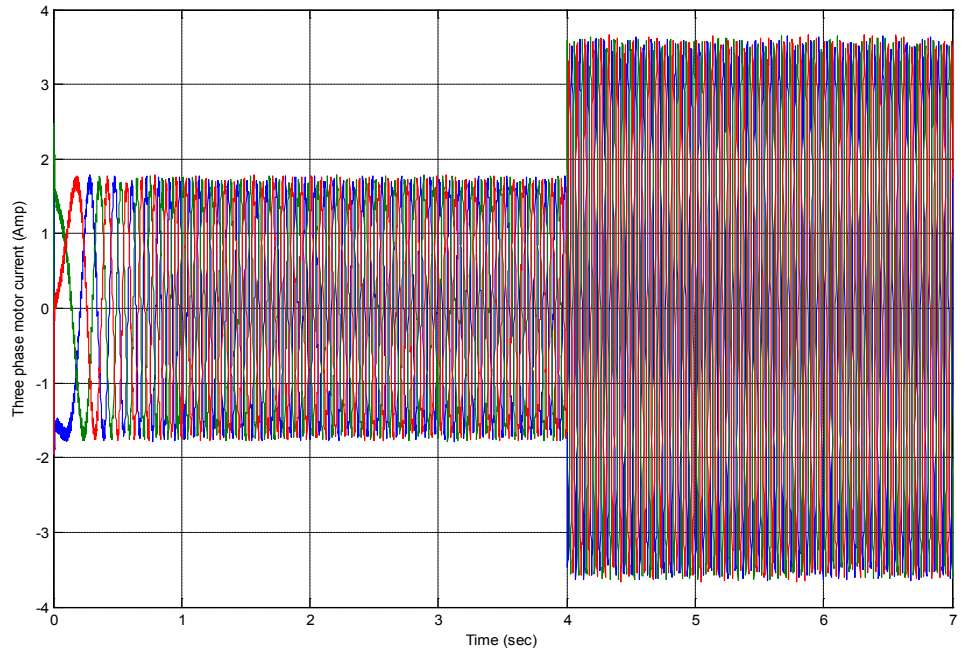
(b)

Figure 4.14 Stator Flux Response (a) FOC (b) DTC

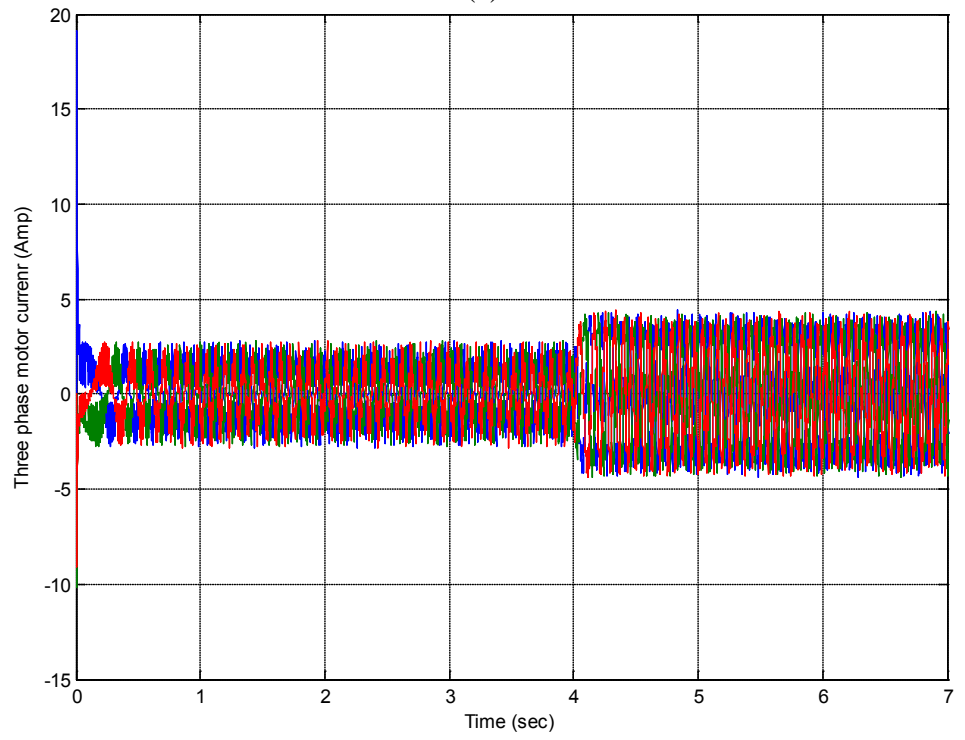
In addition, when the motor is step torque loaded, the flux in (b) stays reaching the desired value with more ripples but in FOC (a) the flux decreases under the desired value with fewer ripples (0.76-0.78) Wb.

4.5.1.4 Three phase current drive Comparison

The resultant three phase current in FOC and DTC models are shown in Fig 4.14 (a) and (b) respectively. It can be noticed that (b) has a higher transient current which is 19.14 A, but when the motor is loaded the current are reaching the nominal current (4.5 A) smoothly. In contrast when the motor is loaded, the current in FOC is reaching the normal current immediately, and sometimes little spiky current if the motor is heavily loaded. The normal current when the motor is loaded is 3.67A.



(a)



(b)

Figure 4.15 Three phase motor current (a) FOC (b) DTC

4.5.1.6 Discussing my simulation results and comparing them to other studies

The summary of the comparison between FOC and DTC when the motor is loaded in its steady state operation status as follows:

- FOC has a better speed response than DTC, whereas the speed in FOC is not significantly affected by the load
- FOC has faster torque response and less ripples than DTC but DTC does not exceed the desired torque as much as FOC does. The latter action could be problem to draw high current especially when the motor is overloaded sometimes or the torque load is pulsating torque as it is shown in Fig 4.16.
- DTC has much faster and more stable flux response and that is due to the hysteresis band that keeps the flux within the desired band.
- The RMS value of the three phase current of DTC is higher and more distorted than the three phase current in FOC as we can clearly notice in Fig 4.17 when both models are designed to run at the same desired speed and the same load torque are applied on them.
- DTC is known to be less complicated to simulate and implement because of the absence of the vector transformation which is used in FOC in decoupling part. That can be noticed when we take a look at the two models in Appendixes B and D and when they are built experimentally.
- DTC and FOC are both affected by the parameters varying of the parameters. DTC is affected by the variation of the stator resistance because the stator flux selection is based on the equation $\lambda_s = \int (V_s - r_s i_s) dt$. FOC technique is affected by the rotor time constant $\tau_r = L_r / r_r$ and those are changed by the temperature and the flux level.

- Those comparisons agree with the comparison which was done in the studies [18], [19] and [27].

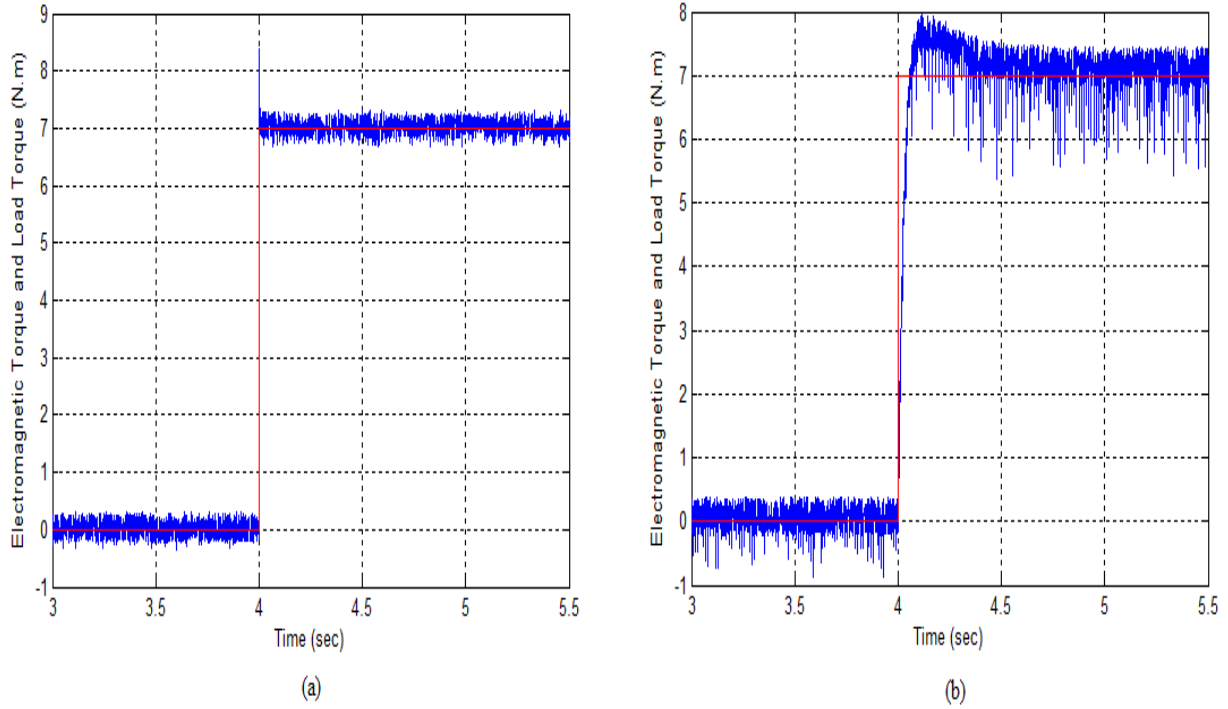


Figure 4.16 Torque responses (a) FOC (b) DTC.

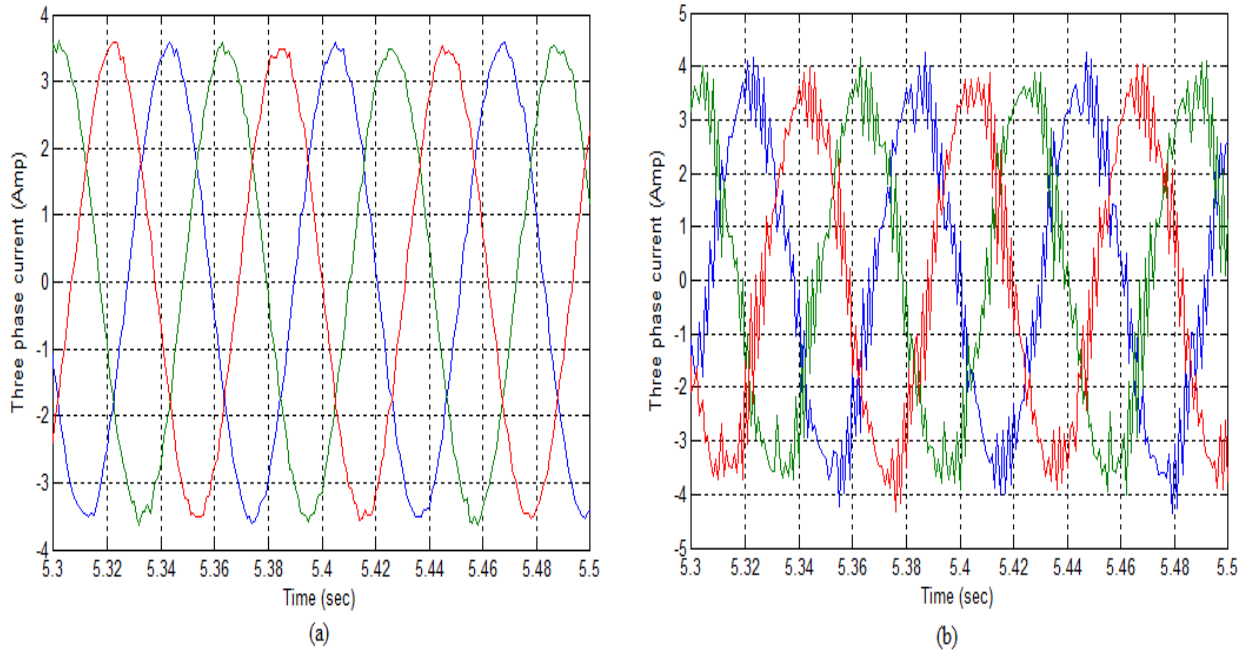


Figure 4.17 The distortion of Three phase current (a) FOC (b) DTC.

4.5.2 Simulation Results in the presence of Voltage-Sag and Short Interruption

Eight power quality issues, which the induction motors are affected by are voltage sag, short interruption, harmonics, unbalance, impulse surges, overvoltage, and undervoltage [28]. The driving systems of the AC motors are primarily sensitive to the voltage-sags and short interruptions, so it is worth a while to test the two driving techniques that are used in this thesis project which are FOC and DTC. In this section, the effect of these power quality issues on the DC link voltage, speed and torque is explained. The characteristics of the voltage sag and short interruption are explained. Finally, the simulation results and the behavior of the two methods are presented.

4.5.2.1 The effect of Voltage sags and short interruption on driven induction motors

Adjustable Speed Drive (ASD) is considered as one of the sensitive loads to the voltage sag and short interruption and that might cause the motor protection relay to trip, because the undervoltage of the DC link. The ac current, which is feeding the motor, increases. The speed usually deviates and the torque varies [29].

4.5.2.2 The characteristics of the voltage sag and short interruption

A short interruption is categorized as losing less than 10% of the normal voltage (one phase or more) for duration of 8.333 ms to 3 s. The cause of this problem could be heavily loaded machines, rigorous hot-load pickup and others. Voltage sag itself is characterized as a reduction in the voltage magnitude by 70% to 80% with duration shorter than or equal to 10 cycles [30].

There are both single phase to ground and phase-to-phase faults (unbalanced) sags and three phase (balanced) sags. While balanced voltage sag only has one type of characteristic to it (4), unbalanced sags have three dominate sag characteristics seen in 4.6 to 4.8. A single-phase fault

will cause the faulted phase to drop, but it will also cause the non-faulted phases to drop. It would be assumed that the non-faulted phases would also be affected; however, this is not the case and can be observed on the phasor diagram figure 4.19 type B [29]. In each situation V_{sag} is a vector with both a magnitude and a phase angle associated with it. However, in 4.6 it is assumed that there is only an effect on the magnitude of the phase and not its angle. Each phase can be modeled as such:

$$\begin{aligned}
 V_a &= V_{SAG} \\
 V_b &= -\frac{1}{2} - \frac{1}{2} \times i\sqrt{3} \\
 V_c &= -\frac{1}{2} + \frac{1}{2} \times i\sqrt{3}
 \end{aligned} \tag{4.6}$$

A phase-to-phase fault will cause the two-faulted phase to pull towards each other when occurring in a wye-connected load. This is referred to as a phase ‘jump’ and is a phenomenon observed not only in the magnitude of the phase, but also in its angle during the duration of the fault. It would be assumed that the non-faulted phase would also be affected in this scenario. However, this is not the case for the non-faulted phase remains at 1 PU and can be seen in figure 1 type C [10]. In the case of a fault across the b and c phase of the system:

$$\begin{aligned}
 V_a &= 1 \\
 V_b &= -\frac{1}{2} - \frac{1}{2} \times V_{SAG} \times i\sqrt{3} \\
 V_c &= -\frac{1}{2} + \frac{1}{2} \times V_{SAG} \times i\sqrt{3}
 \end{aligned} \tag{4.7}$$

With the same phase-to-phase fault on a delta connected load, the phasor diagram takes on a much different orientation. The two faulted phases will pull toward the non-faulted phase, and all three phases will experience a decrease in magnitude, Fig 4.19 type F [29].

The final type of voltage sag this thesis considers is balanced sag. This occurs when all three phases experience a sag and the characteristics of this sag are all three phases drop with the

same magnitude as their counter parts, but there will not be a phase shift involved seen in Fig 4.19 type A and (4.8) [29]. For this study only types A and B, phase to ground and three-phase voltage sag respectively, will be studied.

$$\begin{aligned}
 V_a &= V_{SAG} \\
 V_b &= -\frac{1}{2} - \frac{1}{2} \times V_{SAG} \times i\sqrt{3} \\
 V_c &= -\frac{1}{2} + \frac{1}{2} \times V_{SAG} \times i\sqrt{3}
 \end{aligned}
 \tag{4.8}$$

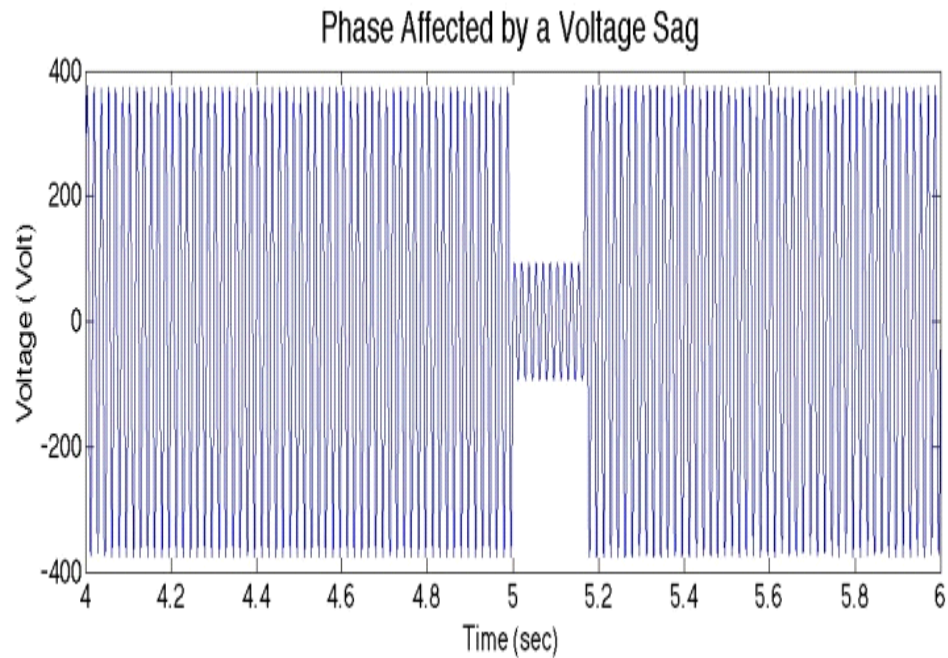


Figure 4.18 Single Phase under Voltage Sag Conditions

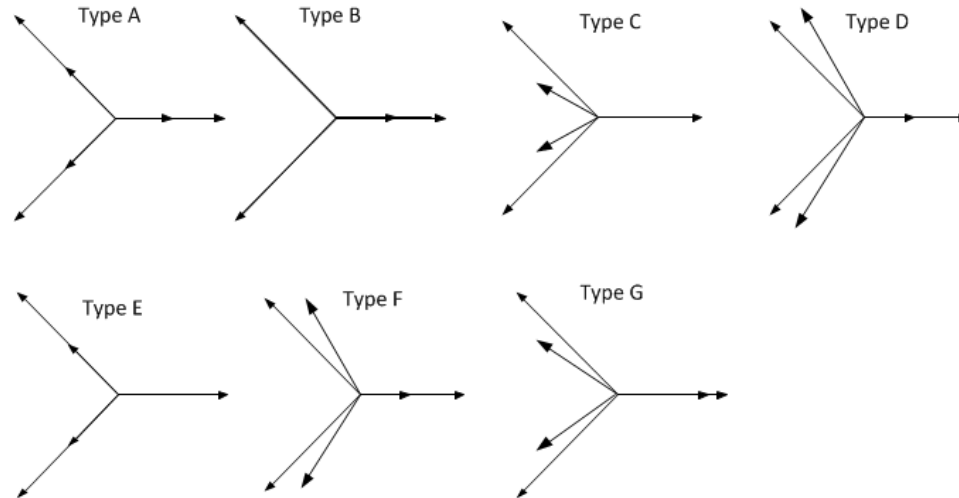


Figure 4.19 Voltage Sag Phasor Diagrams
 Recreated directly without permission from [29]

The voltage sag types, which are used in this project thesis, are Type A (Balanced) and Type B (Unbalanced). The short interruption is applied on the two driving techniques too.

4.5.2.3 Simulation Results

In this section, the effect of voltage-sags (Type A and Type B) and short interruption on DC link is studied and results outlined. Also the effect on the torque variation and speed deviation is studied in different voltage sag depth conditions for both driving techniques. A three phase rectifier circuit was used and apply an opposite voltage to get the voltage Sag (Types A and B) and short interruption (when the Voltage Sag is higher than 90%). It was assumed that the voltage Sag or short interruption happens at 5.5 second and the motor is fully loaded (worst case). The effect of the duration (5, 15 and 60 cycles) of three phase short interruption on the DC link voltage is shown as an example in Fig 4.12

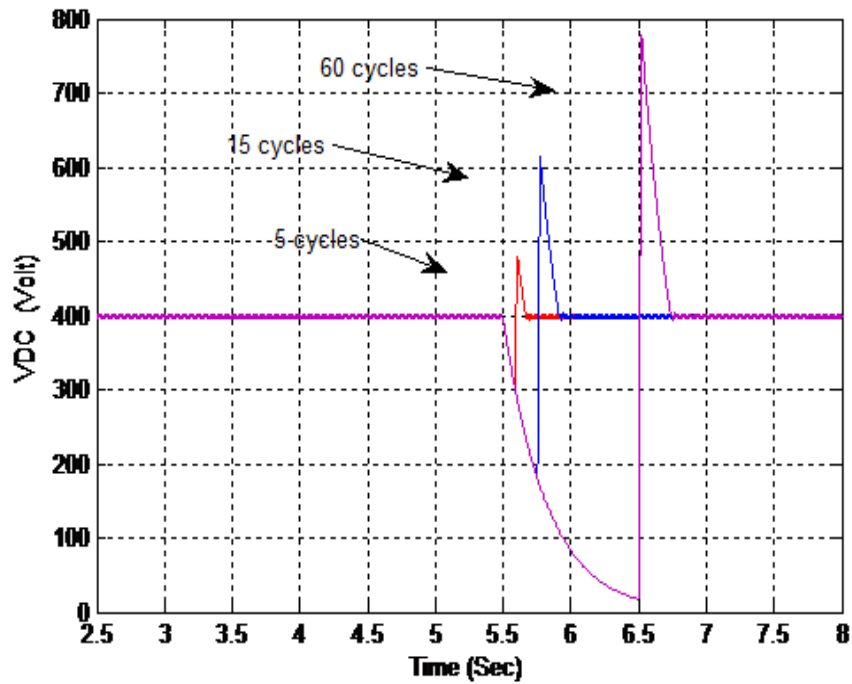


Figure 4.20 The effect of the duration of the three phase short interruption on DC Voltage.

That was the worst case that the driven induction motor could face, which is considered as Type A. Fig 4.21 shows the DC voltage when the short interruption happens in one phase only. It is noticed that the effect is shown as some ripples around the desired DC voltage value.

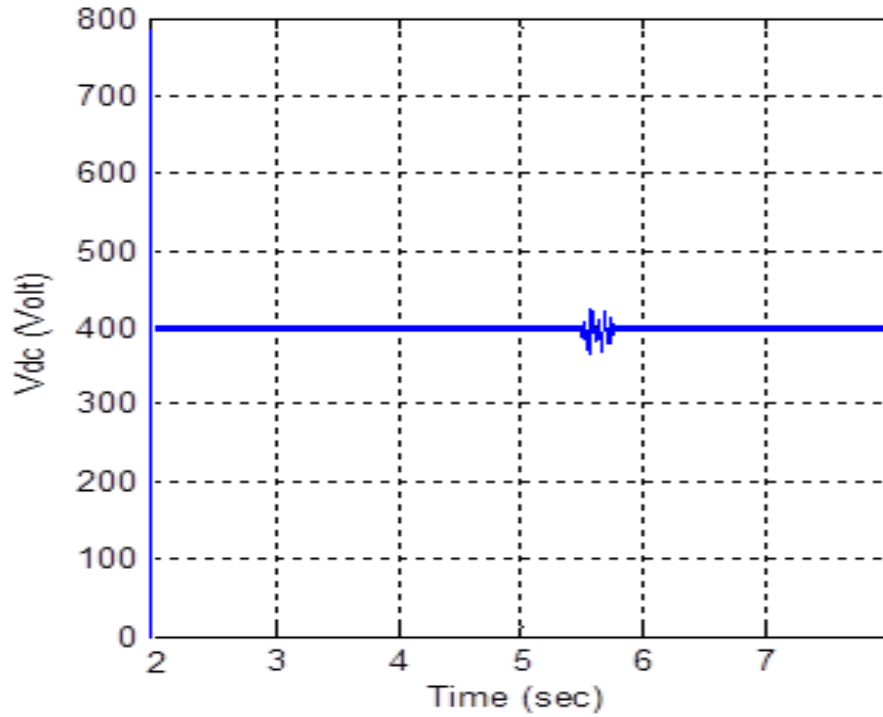


Figure 4.21 One phase short interruption's effect on DC link voltage (Type B)

The effect of 75% of voltage sag for 10 cycle's duration is shown in Fig 4.19 as an example and the effect is taking the same shape but with different voltage drop values.

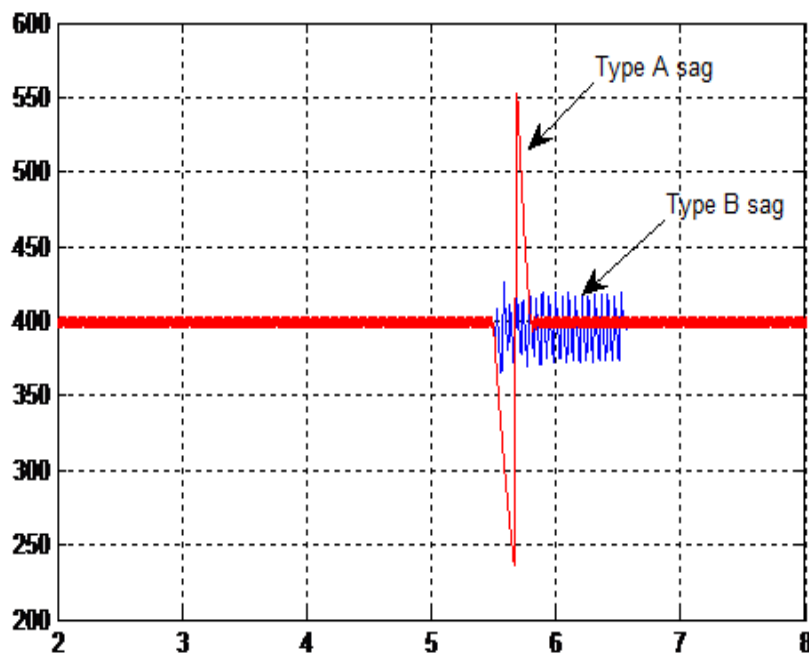


Figure 4.22 DC voltage wave shape under the effect of two types of voltage sag condition

4.5.2.3.1 The effect of the Voltage dip and short interruption taken in different duration and different sag percentage

The driven motor models, using FOC and DTC, are studied under the effect of voltage sag and short interruptions (both type A and type B). The outputs to be observed are the DC link voltage, which is the output of three phase full wave Rectifier Bridge and the input of the inverter, the speed deviation of the motor, torque variation, and obviously the motor current.

For type B, when the sag or interruption occurs in one phase only, both models (FOC and DTC) and the output are not affected, except merely increasing the ripples in the DC voltage as is shown in Fig 4.21. The speeds, torque, motor current are not affected until 3 seconds and the motor is fully loaded in the case of interruption referring to [30] for specifying the duration.

For type A, the voltage sag is applied on both models at different durations (18, 22, 26, and 30) cycles and different sag percentages (20, 40, 60, and 80) %. Short interruption is also applied in the same time durations. The reason to start with 18 cycles is that both models start to be affected from this duration. The observations of the DC link voltage, speed drop, and the motor current are summarized as follows:

- The DC voltage is inversely proportional with the voltage sag or interruption and the duration and that is obviously for both techniques and we can notice that if we look at Appendix E part (I). When the sag or the interruption is removed, the voltage spikes and then it stays normal at the desired voltage value (400Volt in this case).
- The effect of sags and interruptions on speed is slightly different in both techniques. In FOC, the speed starts to drop significantly from (70% and 22 cycles) and the drop of the speed keeps to be gradually deeper when the sag percentage increases and the duration increases. For more information, look at Appendix E part (II). In DTC, on the other hand, the speed stays as the desired speed with a little bit of distortion

$\pm 1.5\%$ till it comes to point the motor speed reaches zero and the motor stalls as we can notice in part (III).

- The effect on the motor current is due to the torque spike after the effective sag or interruption removed. That causes the current to increase at the same time in FOC and that is dangerous and the hardware system has to have over current protection. In DTC, the sag or interruption which causes the motor to stall is causing the motor current to drop and to be distorted. Look at Appendix E parts (IV and V).

CHAPTER 5

CONCLUSION AND FUTUER WORK

5.1 Conclusion

In this thesis project, two induction motor drive techniques (FOC and DTC) are first studied theoretically by using MATLAB/SIMULINK. We also explain the basic principles of those two differing methods and the mathematical representations and the needed operation to achieve the high performance control. Those methods are compared using MATLAB/SIMULINK in two grid disturbance different cases. The first case compares them when there is no voltage sags or short interruptions, i.e. the normal operation. The second case is when the common short interruption or voltage sag fault occurs. We determined how sensitive those methods are to those kinds of faults.

In the normal operation case, the speed response resultant from the FOC is faster and more robust than the DTC. The DTC technique has a better torque response, which is following the load torque smoothly instead of having the torque overshoot to a higher value than the required. That is a distinct disadvantage, because of the higher current that the motor must draw. The DTC has a faster stator magnetic flux response and when the motor is loaded the stator keeps following the flux band that is desired. In contrast, in the FOC technique the stator flux is slowly reaching the desired value and when the motor is loaded it might deviate from the desired values, especially the fully mechanical loaded case. DTC is easier to implement but FOC is more complicated because of the coordinate transformation which helps in the decoupling control. Thus, it is hard to definitely say that DTC is better than FOC each of the techniques has the excellence in some of the comparison aspects on the other. In general each technique has advantages and disadvantages, so we cannot say that one of them is completely better than the other but that is based on particular application.

In the presence of the voltage sags or short interruption, both techniques display robustness under the effect of these power quality issues. DTC stays unaffected till a point of voltage sag or short interruption that can cause the motor speed to drop to zero. At that point the motor stalls and the advantage of this stall, is that the motor is not going to draw a higher current. In FOC case the speed starts to drop at earlier point than the point (sag percentage and duration) in DTC and that causes the motor to demand much higher torque after the sag or interruption is removed. The bad consequences are that the motor is going to demand very high current that damages the electronics and still stalls the motor. Again, it is hard to say that one technique is preferred to the other. This study has shown that the driven motor behavior is improved by both methods, not only in performance but also under the voltage sags and short interruption.

5.2 Recommended Future Work

The future work on this topic should continue to do more detailed analysis in comparing those two important methods. Real time simulation should be done and conduct full analysis of the other power quality issues such as harmonic analysis, other voltage sag types and short interruption and others. In addition simulation should take into consideration the protection system for both under voltage and overvoltage. Only a few simulation comparison studies between those techniques are reported and study the performance of the torque, flux, and speed. Future studies should focus more on power quality issues and that should be done as experimental study to verify if the motor modeling is matching the motor performance. Recently, a small driving station lab completed at CSU to be used in a new course ECE 462 for education purposes. There is a second plan to get this small driving station lab modeled as a real time simulation.

REFERENCES

- [1] A. M. Trzynadlowski, *Control of induction motors*: Academic Pr, 2001.
- [2] C. M. Ong, *Dynamic simulation of electric machinery: using MATLAB/SIMULINK* vol. 5: Prentice Hall PTR Upper Saddle River, NJ, 1998.
- [3] W. Theodore, *Electrical Machines, Drives And Power Systems, 6/E*: Pearson Education India, 2007.
- [4] P. Vas, *Vector control of AC machines*: Clarendon press Oxford, 1990.
- [5] N. Mohan and T. M. Undeland, *Power electronics: converters, applications, and design*: Wiley-India, 2007.
- [6] T. Gonen, *Electrical Machines With Matlab*: CRC Press, 2011.
- [7] K. S. Gaeid, H. W. Ping, and H. A. F. Mohamed, "Simulink representation of induction motor reference frames," 2009, pp. 1-4.
- [8] J. A. Santisteban and R. M. Stephan, "Vector control methods for induction machines: an overview," *Education, IEEE Transactions on*, vol. 44, pp. 170-175, 2001.
- [9] X. Wang, Y. Yang, and W. Liu, "Simulation of vector controlled adjustable speed System of induction motor based on Simulink," 2011, pp. 2563-2566.
- [10] R. Lee, P. Pillay, and R. Harley, "D, Q reference frames for the simulation of induction motors," *Electric power systems research*, vol. 8, pp. 15-26, 1984.
- [11] S. Masoudi, M. R. Feyzi, and M. Sharifian, "Speed control in vector controlled induction motors," 2009, pp. 1-5.
- [12] K. Shi, T. Chan, and Y. Wong, "Modelling of the three-phase induction motor using SIMULINK," 1997, pp. WB3/6.1-WB3/6.3.
- [13] A. Diaz, R. Saltares, C. Rodriguez, R. Nunez, E. Ortiz-Rivera, and J. Gonzalez-Llorente, "Induction motor equivalent circuit for dynamic simulation," 2009, pp. 858-863.
- [14] A. Iqbal, A. Lamine, and I. Ashra, "Matlab/Simulink Model of Space Vector PWM for Three-Phase Voltage Source Inverter," 2006, pp. 1096-1100.
- [15] F. M. Abdel-kader, A. El-Saadawi, A. Kalas, and O. M. EL-baksawi, "Study in direct torque control of induction motor by using space vector modulation," 2008, pp. 224-229

- [16] S. Allirani and V. Jagannathan, "High Performance Direct Torque Control of Induction Motor Drives Using Space Vector Modulation," *International Journal of Computer Science*, vol. 7.
- [17] Y. Tang and G. Lin, "Direct torque control of induction motor based on self-adaptive PI controller," 2010, pp. 1230-1234.
- [18] J. N. Nash, "Direct torque control, induction motor vector control without an encoder," *Industry Applications, IEEE Transactions on*, vol. 33, pp. 333-341, 1997.
- [19] H. Le-Huy, "Comparison of field-oriented control and direct torque control for induction motor drives," 1999, pp. 1245-1252 vol. 2.
- [20] S. Vaez-Zadeh and E. Jalali, "Combined vector control and direct torque control method for high performance induction motor drives," *Energy conversion and management*, vol. 48, pp. 3095-3101, 2007.
- [21] N.Mohan, "First Course on Electric Machines and Drives Videos," 2010: http://cusp.umn.edu/electric_drives.php
- [22] B. M. Wilamowski and J. D. Irwin, "The Industrial Electronics Handbook-Power Electronics and Motor Drives," ed: Taylor and Francis Group, LLC, 2011
- [23] P. Tiitinen and M. Surandra, "The next generation motor control method, DTC direct torque control," 1996, pp. 37-43 vol. 1.
- [24] S. K. Sul, *Control of electric machine drive systems* vol. 88: Wiley-IEEE Press, 2011.
- [25] A. Ansari and D. Deshpande, "Mathematical Model of Asynchronous Machine in MATLAB Simulink," 2010.
- [26] P. Wach, *Dynamics and Control of Electrical Drives*: Springer, 2011.
- [27] D. Telford, M. Dunnigan, and B. Williams, "A comparison of vector control and direct torque control of an induction machine," 2000, pp. 421-426 vol. 1.
- [28] J. C. Gomez, M. M. Morcos, C. A. Reineri, and G. N. Campetelli, "Behavior of induction motor due to voltage sags and short interruptions," *Power Delivery, IEEE Transactions on*, vol. 17, pp. 434-440, 2002.
- [29] J. Pedra, F. Córcoles, and F. Suelves, "Effects of balanced and unbalanced voltage sags on VSI-fed adjustable-speed drives," *Power Delivery, IEEE Transactions on*, vol. 20, pp. 224-233, 2005.

- [30] J. Gomez, M. Morcos, C. Reineri, and G. Campetelli, "Induction motor behavior under short interruptions and voltage sags," *Power Engineering Review, IEEE*, vol. 21, pp. 11-15, 2001.
- [31] M. H. Bollen and I. Gu, *Signal processing of power quality disturbances* vol. 30: Wiley-IEEE Press, 2006.

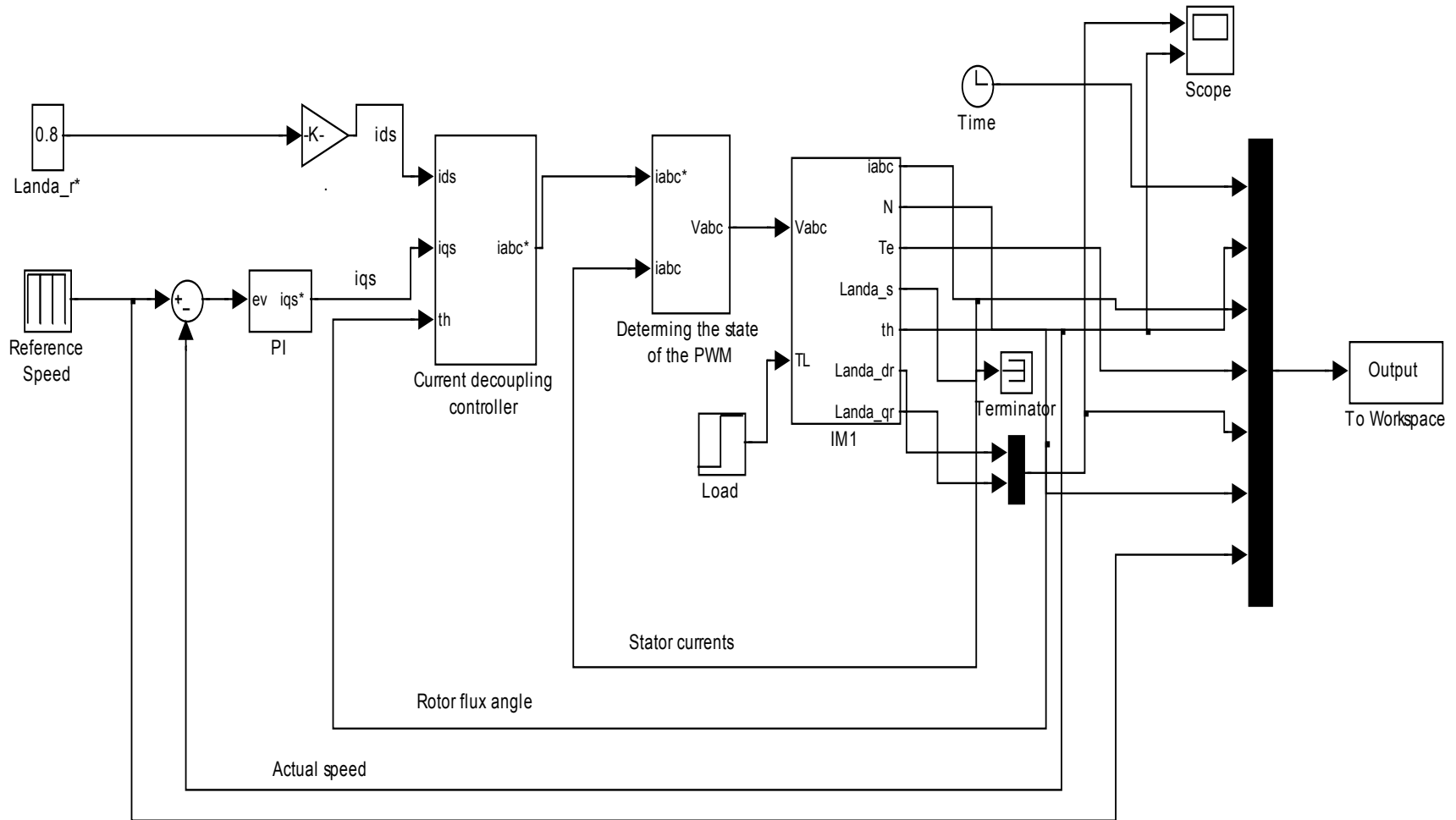
APPENDIX A

Induction Motor parameters

Values	Parameters
$P=1.1 \text{ KW}$	Rated Power
$V_{\text{rated}}=380 \text{ Volt}$	Rates Voltage
$I_{\text{rated}}=2.77 \text{ Amp}$	Rated Current
$R_s = 5.46 \Omega$	Stator Resistance
$R_r = 4.45 \Omega$	Rotor Resistance
$L_s = 0.492 \text{ H}$	Stator Inductance
$L_r = 0.492 \text{ H}$	Rotor Inductance
$L_m = 0.475 \text{ H}$	Magnetizing Inductance
$V_{dc} = 400 \text{ V}$	DC link Voltage
$f = 60 \text{ Hz}$	Frequency
$J = 0.005 \text{ Kg}^2$	Inertia
$B = 0.001 \text{ Kg}^2 / \text{sec}$	Friction
$P = 4$	Number of poles

APPENDIX B

The SIMULINK model of the Field Orientation Control (FOC) of Induction Motor.



APPENDIX C

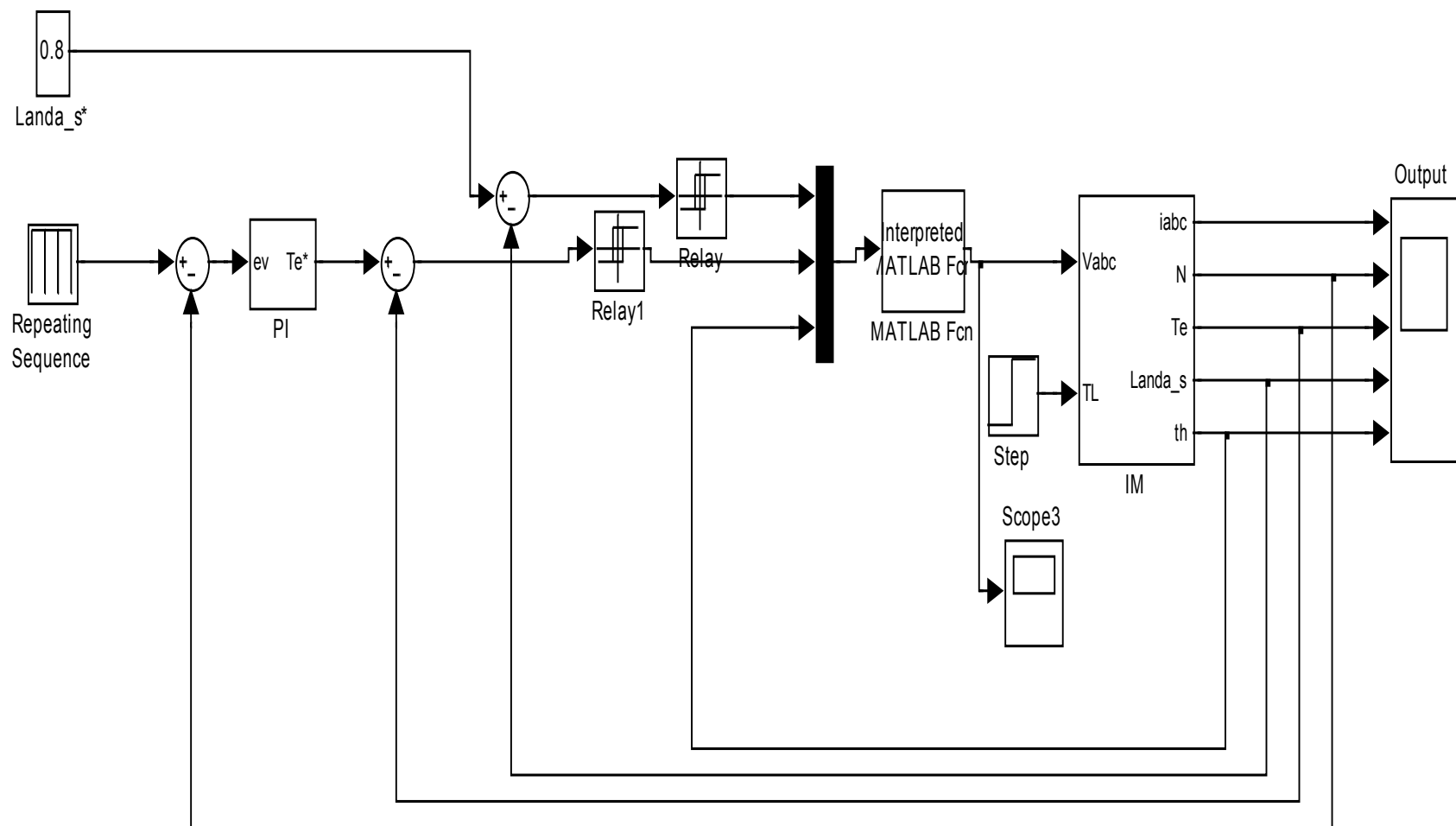
Switching Table Code

```
function [v]=DTC(e);
Vdc=400;
efi=e(1);
ef=e(2);
th=e(3);
if th<0;
th=th+2*pi;
end;
%=====
ap=[1 0 0]; an=[0 1 1]; bp=[0 1 0]; bn=[1 0 1]; cp=[0 0 1]; cn=[1 1 0];
v0=[0 0 0]; v1=[1 1 1];
table=[bp cn ap bn cp an;
        v0 v1 v0 v1 v0 v1;
        an bp cn ap bn cp;
        ap bn cp an bp cn;
        v1 v0 v1 v0 v1 v0;
        cp an bp cn ap bn];
%=====
if ef==0;
m=1;
elseif ef==1;
m=3;
else
m=2;
end;
%=====
if (th>=0 & th<(pi/3));
n=1;
elseif (th>=(pi/3) & th<(2*pi/3));
n=2;
elseif (th>=(2*pi/3) & th<=(pi));
n=3;
elseif (th>=pi & th<(4*pi/3));
n=4;
elseif (th>=(4*pi/3) & th<(5*pi/3));
n=5;
else;
n=6;
end;
%=====
if efi==0;
table1=table(1:3,:);
s=table1(m,n*3-2:n*3);
```

```
elseif efi==1;
table1=table(4:6,:);
s=table1(m,n*3-2:n*3);
else
s=[0 0 0];
end;
v=(Vdc/3)*[2 -1 -1;-1 2 -1;-1 -1 2]*s';
```

APPENDIX D

The SIMULINK model of Direct Torque Control (DTC) of Induction Motor.



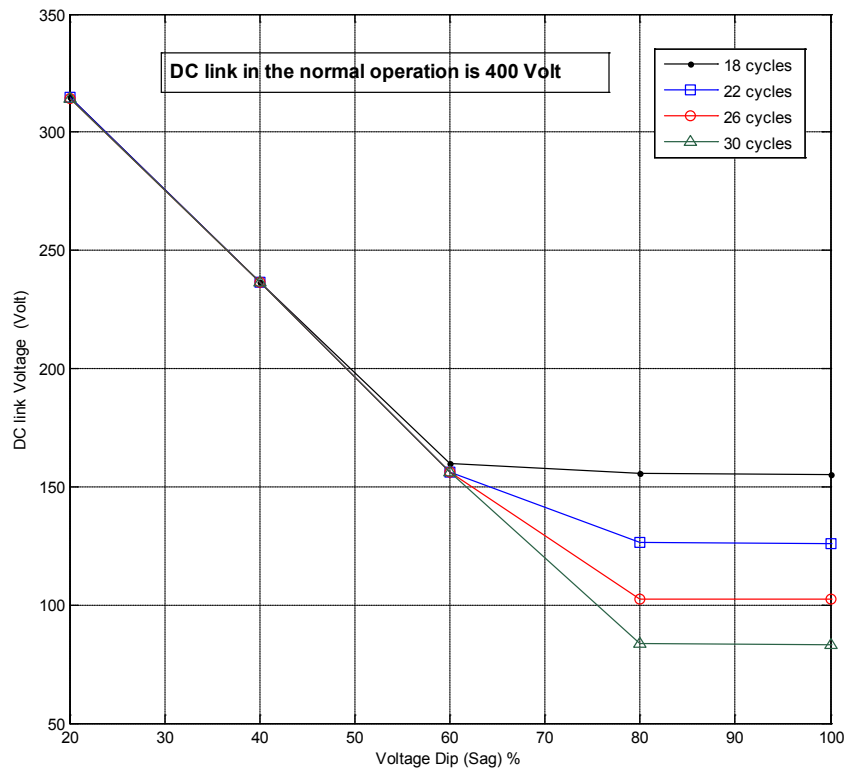
APPENDIX E

The Variation of DC link voltage, speed and motor current due to the Voltage Sag (Type A) and short interruption at different durations in both techniques

I) DC Link Voltage

Table The DC link Voltage in different voltage sag percentages and different durations (Type A)

Sag Duration (Cycles)	18 cycles	22 cycles	26 cycles	30 cycles
Voltages Sag (%)				
20 %	314.75	314.6	314.51	314.2
40 %	236.5	236.4	236.4	236.4
60 %	159.7	156.28	156.26	156.26
80 %	155.4	126.2	102.49	83.55
100 % (interruption)	155.3	126.15	102.4	83.15

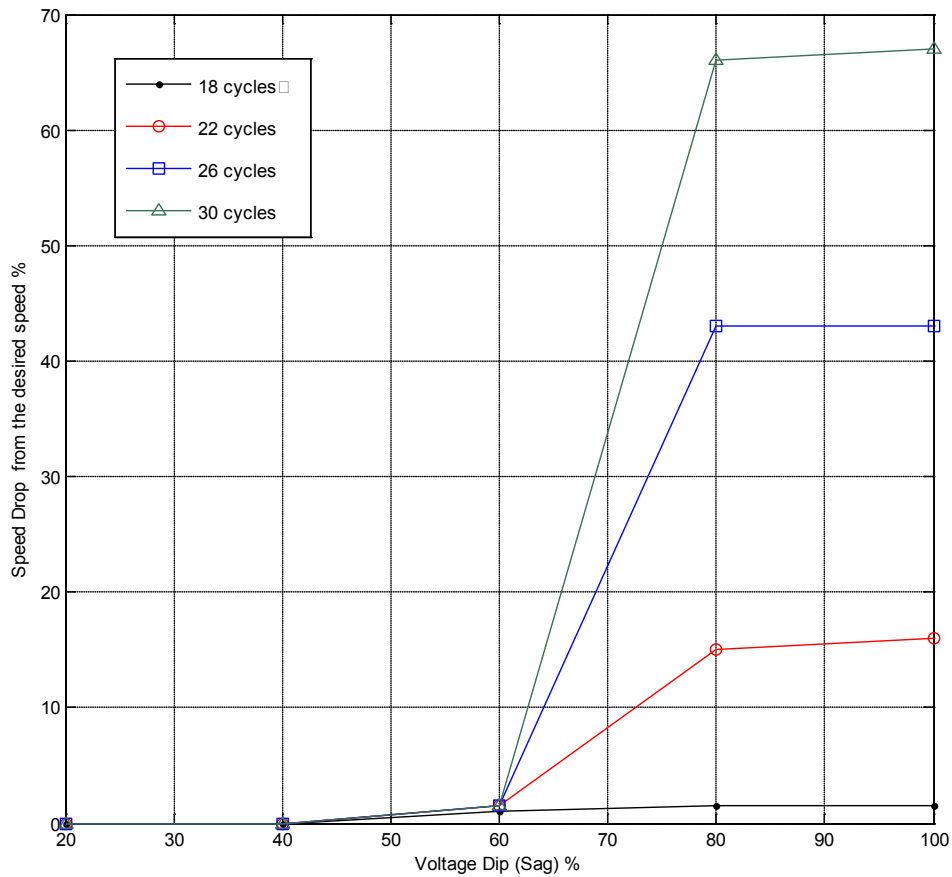


The DC link Voltage in different voltage sag percentages and different durations (Type A)

II) Speed Variation Field Orientation Control (FOC)

Table The speed variation (Drop) in FOC model in the case of (Type A)

Sag Duration (Cycles)	18 cycles	22 cycles	26 cycles	30 cycles
Voltages Sag (%)				
20 %	0%	0%	0%	0%
40 %	0%	0%	0%	0%
60 %	(± 1)%	(± 1.5) %	(± 1.5) %	(± 1.5) %
80 %	(± 1.5) %	(-15, +19) %	(-43,+54) %	(-66, +85) %
100 % (interruption)	(± 1.5)%	(-16, +19) %	(-43,68) %	(-67, +170) %

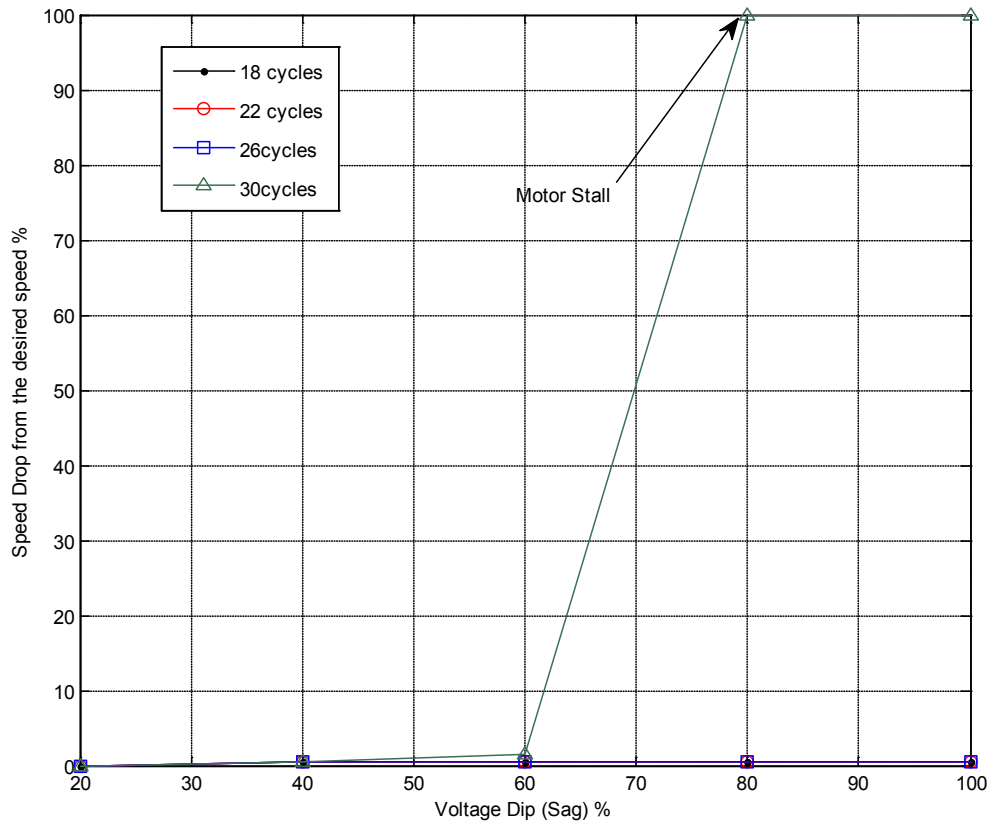


Speed variation (Drop) in FOC model in the case of (Type A)

III) Speed Variation Direct Torque Control (DTC)

Table The speed variation (Drop) in DTC model in the case of (Type A)

Sag Duration (Cycles)	18 cycles	22 cycles	26 cycles	30 cycles
Voltages Sag (%)				
20 %	0%	0%	0%	0%
40 %	(± 0.5) %	(0,+0.5)%	(0,+0.5)%	(0,+0.5)%
60 %	(-0.5, +1) %	(0,+0.5)%	(0,+0.5)%	(± 1.5)%
80 %	(-0.5, +1) %	(-0.5, +1) %	(-0.5, +0.5) %	STALLS
100 % (interruption)	(-0.5, +1) %	(-0.5, +1) %	(-0.5, +1) %	STALLS

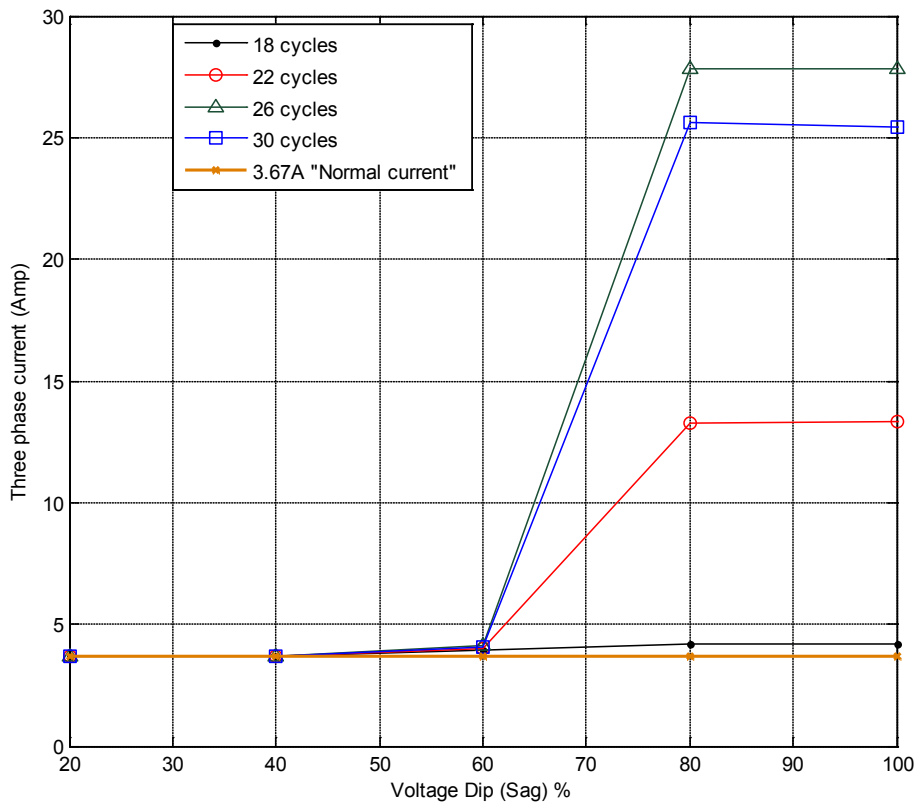


The speed variation (Drop) in DTC model in the case of (Type A)

IV) Peak Current during Voltage Sag applied on FOC

Table The peak three phase current in FOC model in the case of (Type A)
The normal drawn current when the motor is loaded is 3.67 A

Sag Duration (Cycles)	18 cycles	22 cycles	26 cycles	30 cycles
Voltages Sag (%)				
20 %	3.67	3.67	3.67	3.67
40%	3.67	3.67	3.67	3.67
60 %	3.95	3.98	4.1	4.06
80%	4.17	13.28	27.8	25.6
100 % (interruption)	4.19	13.34	27.84	26.45

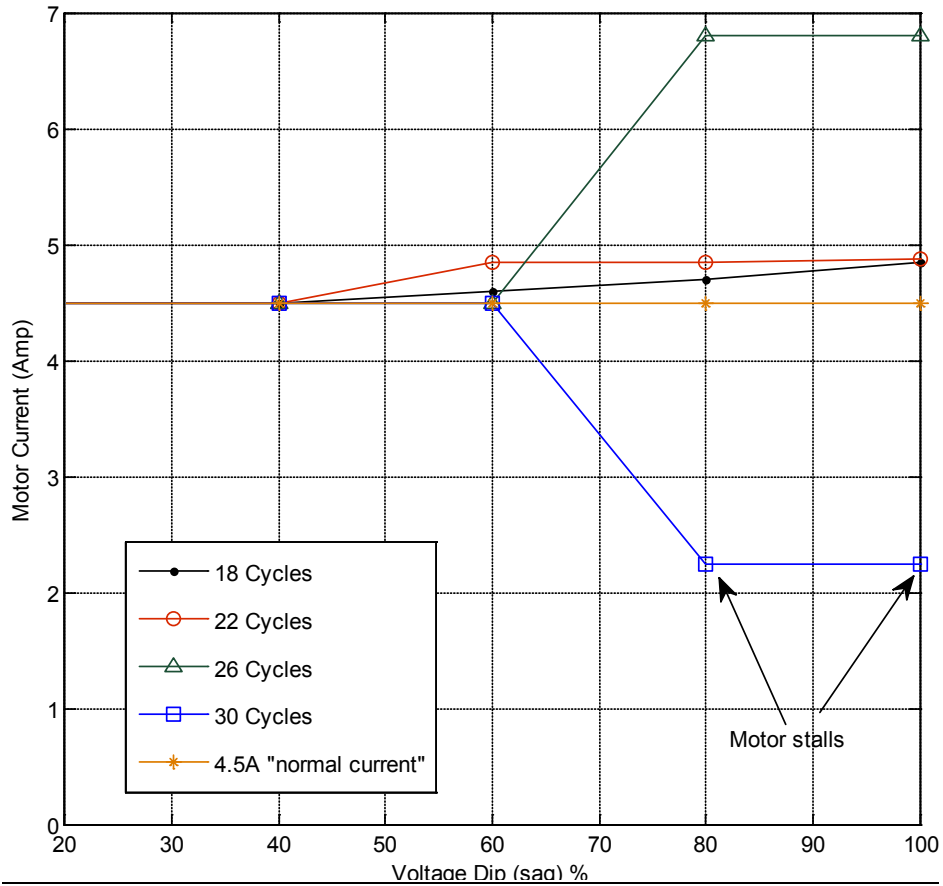


The peak three phase current in FOC model in the case of (Type A)

V) Peak Current during Voltage Sag applied on DTC

Table The peak three phase current in DTC model in the case of (Type A)
The normal drawn current when the motor is loaded is 4.5A

Sag Duration (Cycles)	18 cycles	22 cycles	26 cycles	30 cycles
Voltages Sag (%)				
20 %	4.5	4.5	4.5	4.5
40 %	4.5	4.5	4.5	4.5
60 %	4.6	4.84	4.5	4.5
80 %	4.7	4.84	6.8	1.5-3
100 % (interruption)	4.84	4.87	6.8	1.5-3



The peak three phase current in DTC model in the case of (Type A)